Chapter 3
Elementary Uni-axial Constitutive Models

Basic information on the material behavior is usually obtained from a uni-axial test. The development of a constitutive model for a uni-axial stress state is the first step to the general structural analysis. This is a motivation to apply equations discussed in this chapter to develop constitutive models and to analyze restrictions to the response functions and material properties.

Materials are often subjected to complex thermo-mechanical loading conditions. To analyze material behavior under such conditions a combined model for thermo(visco)elasto-plasticity considering hardening, softening, damage and other processes is required. Such models are proposed and discussed in the literature. The idea of this chapter is to introduce elementary constitutive models, useful for the analysis of material behavior at high temperature.

3.1 Heat Transfer

Assume that the rod is mechanically isolated such that the local power of the internal force $\sigma \dot{F} F^{-1}$ in (2.6.50) is zero. This can be accomplished by keeping the deformation constant, for example, by setting $F = 1$. The internal force N and consequently the stress σ are not zeros and arise as reactions on the kinematical constraint. The inequality (2.6.50) simplifies to

$$-\rho\dot{\Phi} - \rho\mathcal{S}\dot{T} - q\frac{T'}{T} \geq 0 \tag{3.1.1}$$

The independent variables in Eq. (3.1.1) are ρ, T and T'. Instead of the density ρ one may take the change in volume $J = \rho_0/\rho$ as the independent variable. The conjugate variables (sometimes called thermodynamic forces) are S and q. These can be assumed to be the functions of the independent variables, i.e.

© Springer International Publishing Switzerland 2016

K. Naumenko and H. Altenbach, *Modeling High Temperature Materials Behavior for Structural Analysis*, Advanced Structured Materials 28,
DOI 10.1007/978-3-319-31629-1_3

$$S = S(J, T, T'), \quad q = q(J, T, T')$$

Consequently, the free energy Φ has the same arguments

$$\Phi = \Phi(J, T, T')$$

$$\dot{\Phi} = \frac{\partial \Phi}{\partial J}\dot{J} + \frac{\partial \Phi}{\partial T}\dot{T} + \frac{\partial \Phi}{\partial T'}\dot{T}' \tag{3.1.2}$$

With Eq. (3.1.2) the inequality (3.1.1) takes the form

$$-\rho\frac{\partial \Phi}{\partial J}\dot{J} - \rho\left(\frac{\partial \Phi}{\partial T} + \mathcal{S}\right)\dot{T} - \rho\frac{\partial \Phi}{\partial T'}\dot{T}' - q\frac{T'}{T} \geq 0 \tag{3.1.3}$$

Inequality (3.1.3) can be formulated as follows

$$A\dot{J} + B\dot{T} + C\dot{T}' + D \geq 0, \tag{3.1.4}$$

where the coefficients

$$A = -\rho\frac{\partial \Phi}{\partial J}, \quad B = -\rho\left(\frac{\partial \Phi}{\partial T} + \mathcal{S}\right), \quad C = -\rho\frac{\partial \Phi}{\partial T'}, \quad D = -q\frac{T'}{T} \tag{3.1.5}$$

do not depend on the rates of independent variables. For arbitrary $\dot{J}$, $\dot{T}$ and $\dot{T}'$ the inequality is only satisfied if $A = 0$, $B = 0$, $C = 0$ and $D \geq 0$. From

$$\rho\frac{\partial \Phi}{\partial J} = 0, \quad \rho\frac{\partial \Phi}{\partial T'} = 0$$

it follows, that the free energy depends on the temperature only. Furthermore we obtain the constitutive equation for the entropy

$$\mathcal{S} = -\frac{\partial \Phi}{\partial T} \tag{3.1.6}$$

and the inequality

$$-q\frac{T'}{T} \geq 0 \tag{3.1.7}$$

The inequality (3.1.7) is satisfied with the Fourier law of heat conduction

$$q = -\kappa T', \tag{3.1.8}$$

where $\kappa(T) > 0$ is the thermal conductivity. The functions $\kappa(T)$ and $\mathcal{S}(T)$ must be identified experimentally. To discuss the identification procedure let us derive the

heat transfer equation. Neglecting the mechanical power the local energy balance (2.4.38) takes the form

$$\rho A\dot{\mathcal{U}} = -Q' + \rho Ar \tag{3.1.9}$$

With $\mathcal{U} = \Phi + \mathcal{S}T$ and Eq. (3.1.6) the internal energy is the function of the temperature only. For the heat supply r assume the following constitutive equation

$$\rho r = h(T_\mathrm{e} - T), \tag{3.1.10}$$

where $h(T) > 0$ and T_e is the temperature of the environment. Equation (3.1.10) is known as the Newton law of cooling. With Eqs. (3.1.8) and (3.1.10) the energy balance equation (3.1.9) takes the form

$$\rho c(T)\dot{T} = \frac{1}{A}(kAT')' + h(T_\mathrm{e} - T), \quad c(T) = \frac{\mathrm{d}\mathcal{U}}{\mathrm{d}T}, \tag{3.1.11}$$

where $c(T)$ is the heat capacity. For a rod with the constant cross section area this simplifies to

$$\rho c(T)\dot{T} = (kT')' + h(T_\mathrm{e} - T) \tag{3.1.12}$$

Furthermore, assuming that the expected temperature difference is small, one may linearize the temperature functions c, k and h about a reference temperature T_0 leading to the linear differential equation

$$\rho c_0\dot{T} = k_0T'' + h_0(T_\mathrm{e} - T), \tag{3.1.13}$$

where $c_0 = c(T_0)$, $k_0 = k(T_0)$ and $h_0 = h(T_0)$. Equation (3.1.13) is known as the heat equation or diffusion equation. The solution for the given initial condition and the boundary conditions with respect to the heat flux or the temperature provides the time-dependent temperature field in the rod. Several methods exist to identify the functions c, k and h, which are based on temperature measurements and solutions of the heat equation (3.1.13). For details the reader may consult textbooks on heat transfer and thermodynamics, for example, Granger (1994), Müller (2007), Nellis and Klein (2009).

Once the heat capacity $c(T)$ is identified the constitutive equation (3.1.6) allows us to compute the entropy as follows

$$\mathcal{S}(T) = \int_{T_0}^{T} \frac{c(\xi)}{\xi}\mathrm{d}\xi$$

3.2 Thermo-elasticity

Within the framework of elasticity the basic assumption is that the stress is a function of the strain. This can be related to experimental observations from the tensile test, Sect. 1.1. After the loading and subsequent unloading within the elastic range the specimen takes the original length. The elastic behavior is reversible—no hysteresis loop is observable if the specimen is subjected to a closed cycle of strain under adiabatic or isothermal conditions.

Let us assume that the stress and consequently the free energy are functions of the following arguments

$$\sigma = \sigma(F, J, T, T') \quad \Rightarrow \quad \Phi = \Phi(F, J, T, T')$$

Then the inequality (2.6.50) takes the following form

$$\left(\sigma F^{-1} - \rho \frac{\partial \Phi}{\partial F}\right) \dot{F} - \rho \frac{\partial \Phi}{\partial J} \dot{J} - \rho \left(\frac{\partial \Phi}{\partial T} + \mathcal{S}\right) \dot{T} - \rho \frac{\partial \Phi}{\partial T'} \dot{T}' - q \frac{T'}{T} \geq 0 \tag{3.2.14}$$

The left hand side of the inequality (3.2.14) is a linear function of rates of independent variables. Therefore the inequality is satisfied if the following conditions are met (see Sect. 3.1 for a more detailed analysis)

$$\sigma = \rho F \frac{\partial \Phi}{\partial F}, \quad \frac{\partial \Phi}{\partial J} = 0, \quad \mathcal{S} = -\frac{\partial \Phi}{\partial T}, \quad \frac{\partial \Phi}{\partial T'} = 0, \quad -q \frac{T'}{T} \geq 0 \tag{3.2.15}$$

The first condition in Eq. (3.2.15) is the constitutive equation for the stress. With

$$F \frac{\partial \Phi(F)}{\partial F} = \frac{\partial \Phi(\varepsilon_{\mathrm{H}})}{\partial \varepsilon_{\mathrm{H}}}, \quad \varepsilon_{\mathrm{H}} = \ln F = \ln \lambda,$$

where ε_{H} is the Hencky strain (sometimes called true strain) and Eq. (2.2.19) it can be formulated as follows

$$\sigma = \rho \frac{\partial \Phi}{\partial \varepsilon_{\mathrm{H}}} = \frac{\rho}{\rho_0} \frac{\partial \rho_0 \Phi}{\partial \varepsilon_{\mathrm{H}}} = \frac{1}{J} \frac{\partial \rho_0 \Phi}{\partial \varepsilon_{\mathrm{H}}} \tag{3.2.16}$$

From Eqs. (3.2.15) and (3.2.16) it follows that the free energy density must be formulated as a function of the Hencky strain and the temperature. For isothermal conditions, i.e. for $T(x, t) = T_0$ the work done by the stress $J\sigma$ on the infinitesimal change of the Hencky strain is the total differential of the strain energy density function

$$J\sigma \, \mathrm{d}\varepsilon_{\mathrm{H}} = \mathrm{d}(\rho_0 \Phi) \tag{3.2.17}$$

The stress measure $J\sigma$ is called Kirchhoff stress. For adiabatic processes, i.e. for processes without heat transfer with the environment, one may use the local energy balance equation (2.4.38) to show that

$$J\sigma \mathrm{d}\varepsilon_{\mathrm{H}} = \mathrm{d}(\rho_0 \mathcal{U}) \tag{3.2.18}$$

Equations (3.2.17) and (3.2.18) are widely used in the theory of elasticity (Hahn 1985; Lurie 2010; Timoshenko and Goodier 1951) and structural mechanics (Altenbach et al. 1998; Gould 1988; Reddy 1997; Szilard 1974; Timoshenko and Woinowsky-Krieger 1959) for the formulation of variational principles.

The starting point for the analysis was the inequality (2.6.50). One may use the dissipation inequality (2.6.54) defined with respect to the reference configuration to find the relationship between the engineering stress P and the corresponding strain measure. Here we use the first equation in (3.2.15) and the relationship between the stress measures (2.6.55) to derive the following equation

$$P = \frac{\partial \rho_0 \Phi(F)}{\partial F} \tag{3.2.19}$$

To find a particular form of the strain energy density a constitutive equation for the stress is required. For many structural materials, for example steel, the elastic range is observed for small values of strain ε such that $\varepsilon^2 \ll \varepsilon < 1$. Furthermore, in this range the stress is proportional to the strain. In this case it follows $\varepsilon_{\mathrm{H}} \approx \varepsilon$ and Eq. (3.2.15) can be linearized leading to

$$\sigma = \frac{\partial \rho_0 \Phi(\varepsilon)}{\partial \varepsilon} \tag{3.2.20}$$

Furthermore since $\lambda = 1+\varepsilon$ one may use Eq. (3.2.19) to derive the linearized relation for the engineering stress P. Within the linear elasticity the difference between the stress measures is negligible. To find an expression for the free energy density we use the following linear constitutive equation

$$\sigma = E(\varepsilon - \varepsilon^{\mathrm{th}}), \quad \varepsilon^{\mathrm{th}} = \alpha_{\mathrm{th}}\Theta, \quad \Theta = T - T_0, \tag{3.2.21}$$

where E is the Young's modulus and α_{th} is the thermal expansion coefficient. With Eq. (3.2.20)

$$\rho_0 \Phi = \frac{1}{2} E\varepsilon^2 - E\alpha_{\mathrm{th}}\Theta\varepsilon + f(T) \tag{3.2.22}$$

To determine the function $f(T)$ compute

$$\frac{\partial \mathcal{U}}{\partial T} = T\frac{\partial \mathcal{S}}{\partial T} = -T\frac{\partial^2 \oplus}{\partial T^2} \tag{3.2.23}$$

With Eq. (3.2.22) this results in

$$\frac{\partial \mathcal{U}}{\partial T} = \underline{-\frac{1}{\rho_0} T \frac{\mathrm{d}^2 f}{\mathrm{d}T^2}} - \frac{1}{2\rho_0} T \varepsilon^2 \frac{\mathrm{d}^2 E}{\mathrm{d}T^2} - \frac{1}{\rho_0} T \varepsilon \frac{\mathrm{d}^2}{\mathrm{d}T^2} (E \alpha_{\mathrm{th}} \Theta)$$

The underlined term is the heat capacity without deformation, as defined by Eq. (3.1.11). Therefore the function f can be found from the following equation

$$-\frac{1}{\rho_0} T \frac{\mathrm{d}^2 f}{\mathrm{d}T^2} = c(T)$$

With Eqs. (3.1.10), (3.2.22) and (3.2.23) the energy balance equation (2.4.38) takes the following form

$$-\frac{\partial^2(\rho_0 \Phi)}{\partial T^2} \dot{T} - \frac{\partial^2(\rho_0 \Phi)}{\partial T \partial \varepsilon} \dot{\varepsilon} = \frac{1}{A} (k A T')' + h(T_{\mathrm{e}} - T) \tag{3.2.24}$$

Assuming that the expected temperature difference is small one may linearize the functions $E(T)$, $\alpha_{\mathrm{th}}(T)$, $c(T)$ and $h(T)$ about the reference temperature T_0. The heat transfer equation (3.2.24) simplifies to

$$c_0 \dot{T} + E_0 \alpha_{\mathrm{th}_0} \dot{\varepsilon} = \frac{1}{A} (k_0 A T')' + h_0 (T_{\mathrm{e}} - T), \tag{3.2.25}$$

where $E_0 = E(T_0)$ and $\alpha_{\mathrm{th}_0} = \alpha_{\mathrm{th}}(T_0)$. The second term in the left-hand side of Eq. (3.2.25) is usually small and can be neglected (Landau et al. 1986). Therefore, within the linearized theory the deformation has minor influence on the heat transfer such that the heat equation can be solved independently providing the temperature $T(x, t)$. The balance of momentum (2.3.26) with the constitutive equation (3.2.21) yields

$$\rho A \ddot{u} = [E A (u' - \alpha_{\mathrm{th}} \Theta)]'$$

3.3 Non-linear Viscosity, Viscoplasticity, and Rigid Plasticity

Assume that the stress σ is the function of the deformation rate $\dot{F} F^{-1} = \dot{\varepsilon}_{\mathrm{H}}$ and the temperature. Furthermore, assume that the mechanical power $\sigma \dot{F} F^{-1}$ does not influence the free energy directly. The free energy and the entropy are then the functions of the temperature only. Then the inequality (2.6.50) takes the following form

$$-\rho \left(\frac{\partial \Phi}{\partial T} + \mathcal{S} \right) \dot{T} + \sigma \dot{\varepsilon}_{\mathrm{H}} - q \frac{T'}{T} \geq 0 \tag{3.3.26}$$

The inequality (3.3.26) has the form $A(T)\dot{T} + B(T, \dot{\varepsilon}_{\mathrm{H}}) \geq 0$. For arbitrary (positive and negative) rates of temperature it can only be satisfied if $A = 0$ and $B \geq 0$. This leads to the constitutive equation for the entropy

$$\mathcal{S} = -\frac{\partial \Phi}{\partial T} \tag{3.3.27}$$

and the dissipation inequality

$$\sigma \dot{\varepsilon}_{\mathrm{H}} - q\frac{T'}{T} \geq 0 \tag{3.3.28}$$

Assuming that the heat flux q does not depend on the strain rate results in two inequalities

$$\sigma \dot{\varepsilon}_{\mathrm{H}} \geq 0, \quad -q\frac{T'}{T} \geq 0 \tag{3.3.29}$$

For the stress one may assume the constitutive equation in the form

$$\sigma(\dot{\varepsilon}_{\mathrm{H}}, T) = g_{\dot{\varepsilon}_{\mathrm{H}}}(|\dot{\varepsilon}_{\mathrm{H}}|)\mathrm{sgn}(\dot{\varepsilon}_{\mathrm{H}})g_T(T), \tag{3.3.30}$$

where $g_{\dot{\varepsilon}_{\mathrm{H}}}(|\dot{\varepsilon}_{\mathrm{H}}|) \geq 0$ is a function of strain rate with $g_{\dot{\varepsilon}_{\mathrm{H}}}(0) = 0$ and $g_T(T) > 0$ is a function of temperature. Both the functions can be identified from stress-strain diagrams in the saturation (steady state) regime, Fig. 1.2 by taking experimental data for the stress σ_{ss} as a function of the strain rate and the temperature. By inverting Eq. (3.3.31) the constitutive equation for the strain rate can be formulated as follows

$$\dot{\varepsilon}_{\mathrm{H}} = f_\sigma(|\sigma|)\mathrm{sgn}(\sigma)f_T(T), \tag{3.3.31}$$

where $f_\sigma(|\sigma|) \geq 0$ is a function of stress with $f_\sigma(0) = 0$ and $f_T(T)$ is a function of temperature. These functions can be identified from experimental data of secondary (steady-state) creep, Fig. 1.5. To this end the minimum creep rates should be taken from experimental creep curves for different stress and temperature levels. Examples for stress and temperature functions include the power-law function of stress and the Arrhenius function of temperature

$$f_\sigma(\sigma) = \dot{\varepsilon}_0\left(\frac{\sigma}{\sigma_0}\right)^n, \quad f_T(T) = \exp\left(-\frac{Q}{RT}\right), \tag{3.3.32}$$

where ε_0, σ_0, n and Q are constants to be identified from experimental data and R is the universal gas constant. Examples for experimental data are shown in Fig. 1.8 for steels. With functions (3.3.32) the constitutive equation for the strain rate is

$$\dot{\varepsilon}_{\mathrm{H}} = \dot{\varepsilon}_0 \exp\left(-\frac{Q}{RT}\right)\left(\frac{|\sigma|}{\sigma_0}\right)^n \mathrm{sgn}(\sigma) \tag{3.3.33}$$

or in the inverse form

$$\sigma = \sigma_0 \exp\left(\frac{Q}{nRT}\right)\left(\frac{|\dot{\varepsilon}_{\mathrm{H}}|}{\dot{\varepsilon}_0}\right)^{\frac{1}{n}} \mathrm{sgn}(\dot{\varepsilon}_{\mathrm{H}}) \tag{3.3.34}$$

Let us note that constitutive equations (3.3.33) and/or (3.3.34) are applicable for narrow ranges of stress, strain rate and temperature. For example, for metals the activation energy decreases and the power exponent n increases with a decrease of temperature. To capture wide stress and temperature ranges advanced functions are required. Functions of stress (strain rate) and temperature will be discussed in Sect. 5.4.4.

For $n = 1$ the model of a linear viscous fluid follows from Eq. (3.3.34). For large values of n the strain rate sensitivity of stress according to Eq. (3.3.34) becomes negligible. For $n \to \infty$ the constitutive equation of rate-independent plasticity (St. Venant model) with the yield stress $\sigma_{\mathrm{y}} = \sigma_0$ follows from Eq. (3.3.34)

$$\begin{cases} |\sigma| - \sigma_{\mathrm{y}} \le 0, \text{ if } \dot{\varepsilon}_{\mathrm{H}} = 0, \\ \sigma = \sigma_{\mathrm{y}} \mathrm{sgn}\dot{\varepsilon}_{\mathrm{H}}, \text{ if } \dot{\varepsilon}_{\mathrm{H}} \neq 0 \end{cases} \tag{3.3.35}$$

The inverse form of the rigid plasticity model is

$$\dot{\varepsilon}_{\mathrm{H}} = \dot{\lambda}\mathrm{sgn}\sigma \quad \begin{cases} \dot{\lambda} = 0, \text{ if } |\sigma| - \sigma_{\mathrm{y}} < 0, \\ \dot{\lambda} \ge 0, \text{ if } |\sigma| - \sigma_{\mathrm{y}} = 0 \end{cases} \tag{3.3.36}$$

In rheology and theory of materials Eq. (3.3.30) is classified as a constitutive equation for non-linear viscous fluid, or non-linear viscous element, see for example Giesekus (1994), Krawietz (1986), Palmov (1998), Reiner (1969). On the other hand, for large values of n the model (3.3.34) is close to the model of rate-independent plasticity. Functions f_σ and f_T can be formulated such that experimental data including viscous flow and plasticity can be described. Therefore a model like (3.3.30) can be classified as viscoplasticity model. For example, viscoplasticity models proposed by Krempl (1996, 1999) do not contain the yield condition and are based on functions like (3.3.30). This definition of viscoplasticity may contradict again the classification in the rheology, where the viscoplastic model is a connection of viscous and rigid plastic elements.

The inelastic deformation of crystalline materials can be explained by dislocation glide and dislocation climb (Frost and Ashby 1982; Nabarro and de Villiers 1995). The glide motion of dislocations dominates at lower homologous temperatures and higher stress levels, while the climb of dislocations over obstacles is important in high-temperature regimes and moderate stress levels. From this point of view, the model like (3.3.30) can be classified as a model of high-temperature plasticity, as preferred in the materials science, see for example Ilschner (1973). In this book we classify the model like (3.3.30) as a model for high-temperature plasticity.

Multi-axial versions of the Eq. (3.3.30) are used in the analysis of hot deformation processes of metals, for example, friction welding (Schmicker et al. 2013, 2015). Constitutive equation (3.3.31) is used for the structural analysis in the steady-state creep range (Altenbach et al. 2008a; Boyle 2012; Naumenko et al. 2009).

3.4 Elasto-plasticity

Assume that the mechanical power $\mathcal{L} = \sigma \dot{F} F^{-1}$ can be additively decomposed in two parts $\mathcal{L} = \mathcal{L}_\mathrm{s} + \mathcal{L}_\mathrm{d}$ with

$$\mathcal{L}_\mathrm{s} = \sigma_\mathrm{s} \dot{F}_\mathrm{s} F_\mathrm{s}^{-1}, \quad \mathcal{L}_\mathrm{d} = \sigma_\mathrm{d} \dot{F}_\mathrm{d} F_\mathrm{d}^{-1},$$

where σ_s and σ_d are stress-like variables and F_s and F_d are deformation-like variables. Assume that σ_s depends only on the deformation-like variables and the temperature, while σ_d depends on the deformation rates and the temperature.[1] This decomposition is used to define a part of the mechanical power which is dissipated as heat, i.e. $\mathcal{L}_\mathrm{d}$ and can affect the free energy by means of temperature and the remaining part $\mathcal{L}_\mathrm{s}$ which directly affects the free energy and under certain conditions can be stored. For example, this is the case when $\dot{F}_\mathrm{d} = 0$ and $T(x,t) = T_0$, i.e. for isothermal elasticity, as discussed in Sect. 3.2. In Ziegler (1983) $\mathcal{L}_\mathrm{s}$ is called quasi-conservative and $\mathcal{L}_\mathrm{d}$—dissipated parts of mechanical power, respectively. Several approaches to define the corresponding stress and deformation parts are discussed in the literature. For example, one may consider various connections of rheological elements including a spring, a viscous element and a friction element (Krawietz 1986; Palmov 1998). A more general approach is to consider a mixture with several constituents having different properties and volume fractions (Besseling and van der Giessen 1994; Naumenko et al. 2011a). Alternatively, one may assume decompositions for the deformation gradient, rate of strain and/or stress (Besseling and van der Giessen 1994; Khan and Huang 1995; Maugin 1992).

In this section let us apply the so-called iso-stress approach with the following constitutive assumption

$$\sigma_\mathrm{s} = \sigma_\mathrm{d} = \sigma$$

The mechanical power can be given as follows

$$\mathcal{L} = \sigma \dot{F} F^{-1} = \sigma (\dot{F}_\mathrm{s} F_\mathrm{s}^{-1} + \dot{F}_\mathrm{d} F_\mathrm{d}^{-1}) \tag{3.4.37}$$

[1] In general, σ_d may also depend on the deformation-like variables. Here we do not consider such a dependence, for the sake of brevity.

It is obvious, that in the uni-axial case the additive split of power with the iso-stress concept is equivalent to following splits of the deformation-like variables

$$\dot{F}F^{-1} = \dot{F}_{\mathrm{s}}F_{\mathrm{s}}^{-1} + \dot{F}_{\mathrm{d}}F_{\mathrm{d}}^{-1} \quad \Rightarrow \frac{\mathrm{d}}{\mathrm{d}t}\ln F = \frac{\mathrm{d}}{\mathrm{d}t}\ln F_{\mathrm{s}} + \frac{\mathrm{d}}{\mathrm{d}t}\ln F_{\mathrm{d}} \quad \Rightarrow F = F_{\mathrm{s}}F_{\mathrm{d}} \tag{3.4.38}$$

Vice versa, if we assume the multiplicative decomposition of the deformation gradient $F = F_{\mathrm{s}}F_{\mathrm{d}}$, then the additive split of the deformation rates and the additive split of the mechanical power (3.4.37) follow. In rheology this corresponds to the Maxwell model of viscoelasticity or Prandtl model of elastoplasticity, where a spring is connected with a dashpot or a friction element in series. For general multi-axial deformation states the multiplicative decomposition of the deformation gradient does not provide the additive decomposition of the deformation rates and the mechanical power, see for example, Besseling and van der Giessen (1994), Khan and Huang (1995), Xiao et al. (2006). Multi-axial constitutive assumptions will be discussed in Chap. 5. To illustrate basic ideas let us skip (3.4.38) and start with the iso-stress constitutive assumption which can be given in the following form

$$\sigma = \sigma_{\mathrm{s}}(F, F_{\mathrm{s}}, F_{\mathrm{d}}, T) = \sigma_{\mathrm{d}}(\dot{F}, \dot{F}_{\mathrm{s}}, \dot{F}_{\mathrm{d}}, T) \tag{3.4.39}$$

If constitutive equations for σ_{s} and σ_{d} are specified then Eq. (3.4.39) can be used to eliminate one of the kinematic variables, for example F_{s}. Indeed, assume that F, F_{d} and T are given as functions of time. Then Eq. (3.4.39) is the first-order ordinary differential equation with respect to F_{s}. It can be solved providing F_{s} as a function of remaining variables and time. Therefore the mechanical power can be decomposed as follows

$$\begin{aligned} &\mathcal{L} = \mathcal{L}_{\mathrm{s}} + \mathcal{L}_{\mathrm{d}}, \\ &\mathcal{L}_{\mathrm{s}} = \sigma(F, F_{\mathrm{d}}, T)\dot{F}F^{-1} - \sigma(F, F_{\mathrm{d}}, T)\dot{F}_{\mathrm{d}}F_{\mathrm{d}}^{-1}, \\ &\mathcal{L}_{\mathrm{d}} = \sigma(\dot{F}, \dot{F}_{\mathrm{d}}, T)\dot{F}_{\mathrm{d}}F_{\mathrm{d}}^{-1} \end{aligned} \tag{3.4.40}$$

Therefore we can assume that the free energy is now a function of three variables F, F_{d} and T. The inequality (2.6.50) can be written as follows

$$\begin{aligned} \left(\sigma F^{-1} - \rho\frac{\partial \Phi}{\partial F}\right)\dot{F} - \left(\sigma F_{\mathrm{d}}^{-1} + \rho\frac{\partial \Phi}{\partial F_{\mathrm{d}}}\right)\dot{F}_{\mathrm{d}} - \rho\left(\frac{\partial \Phi}{\partial T} + \mathcal{S}\right)\dot{T} \\ + \sigma\dot{F}_{\mathrm{d}}F_{\mathrm{d}}^{-1} - q\frac{T'}{T} \geq 0 \end{aligned} \tag{3.4.41}$$

The first line in Eq. (3.4.41) is a linear function of rates of the assumed independent variables. Therefore with procedures discussed in Sects. 3.1 and 3.2 the inequality (3.4.41) can be satisfied with

$$\sigma F^{-1} = \rho\frac{\partial \Phi}{\partial F}, \quad \sigma F_{\mathrm{d}}^{-1} = -\rho\frac{\partial \Phi}{\partial F_{\mathrm{d}}}, \quad \mathcal{S} = -\frac{\partial \Phi}{\partial T} \tag{3.4.42}$$

and

$$\sigma \dot{F}_{\mathrm{d}} F_{\mathrm{d}}^{-1} \geq 0, \quad -q \frac{T'}{T} \geq 0 \tag{3.4.43}$$

From the first and the second equation in (3.4.42) it follows

$$\sigma = \rho \frac{\partial \Phi}{\partial F} F = -\rho \frac{\partial \Phi}{\partial F_{\mathrm{d}}} F_{\mathrm{d}} \tag{3.4.44}$$

or

$$\frac{\partial \Phi}{\partial F} F + \frac{\partial \Phi}{\partial F_{\mathrm{d}}} F_{\mathrm{d}} = 0 \tag{3.4.45}$$

Equation (3.4.45) provides a restriction to the free energy and can be solved by the method of characteristics (Courant and Hilbert 1989). Indeed, the characteristic system of (3.4.45) is

$$\frac{\mathrm{d}F}{\mathrm{d}s} = F, \quad \frac{\mathrm{d}F_{\mathrm{d}}}{\mathrm{d}s} = -F_{\mathrm{d}}, \tag{3.4.46}$$

where s is a time-like variable. Two ordinary differential equations (3.4.46) possess one integral. To formulate it rewrite the second equation in Eqs. (3.4.46) as follows

$$\frac{\mathrm{d}F_{\mathrm{d}}^{-1}}{\mathrm{d}s} = -\frac{1}{F_{\mathrm{d}}^2} \frac{\mathrm{d}F_{\mathrm{d}}}{\mathrm{d}s} = F_{\mathrm{d}}^{-1}, \tag{3.4.47}$$

Now multiply the first equation in (3.4.46) with F_{d}^{-1} and the Eq. (3.4.47) with F and subtract leading to

$$\frac{\mathrm{d}}{\mathrm{d}s}(F F_{\mathrm{d}}^{-1}) = 0 \quad \Rightarrow \quad F F_{\mathrm{d}}^{-1} = C,$$

where C is an integration constant. Therefore $F F_{\mathrm{d}}^{-1}$ is the integral curve of the free energy and

$$\Phi(F, F_{\mathrm{d}}) = \Phi(F F_{\mathrm{d}}^{-1})$$

With Eq. (3.4.44) the stress is given as follows

$$\sigma = \rho \frac{\partial \Phi}{\partial F} F = \rho \frac{\partial \Phi}{\partial F F_{\mathrm{d}}^{-1}} F F_{\mathrm{d}}^{-1} \tag{3.4.48}$$

By specifying $F^{\mathrm{el}} = F F_{\mathrm{d}}^{-1}$ we can formulate the thermoelasticity constitutive equations as it made in Sect. 3.2

$$\sigma = \rho \frac{\partial \Phi(F^{\mathrm{el}})}{\partial F^{\mathrm{el}}} F^{\mathrm{el}} = \rho \frac{\partial \Phi(\varepsilon_{\mathrm{H}}^{\mathrm{el}})}{\partial \varepsilon_{\mathrm{H}}^{\mathrm{el}}}, \quad \mathcal{S} = -\frac{\partial \Phi}{\partial T}, \tag{3.4.49}$$

where $\varepsilon_{\mathrm{H}}^{\mathrm{el}} = \ln F^{\mathrm{el}}$ is the elastic strain. Note the strain in the continuum mechanics is usually understood as a quantity that can be related to the deformation gradient, for example $\varepsilon_{\mathrm{H}} = \ln F$. In this sense the "elastic strain" can only be identified as a strain if $F_{\mathrm{d}} = 1$. Nevertheless, "elastic strain" is convenient to analyze and identify experimental data, for example initial strain in a strain versus time curve or elastic strain part in a stress-strain hysteresis loop, see examples presented in Sect. 1.1.1.

F_{d} can also be defined as a "plastic transformation" (Bertram 2012). The quantity $\varepsilon_{\mathrm{H}}^{\mathrm{pl}} = \ln(F^{\mathrm{pl}})$ can be called the "plastic strain", i.e. a strain upon an artificial unloading such that $F^{\mathrm{el}} = 1$. Again "plastic strain", "creep strain" or "inelastic strain" are useful to identify constitutive models, response functions and material properties from various tests, see Sect. 1.1.1. To define the plastic (inelastic) strain a kinetic equation is required. For example, one may use Eq. (3.3.31)

$$\dot{\varepsilon}_{\mathrm{H}}^{\mathrm{pl}} = f_\sigma(|\sigma|)\mathrm{sgn}(\sigma) f_T(T) \tag{3.4.50}$$

Let us note, that a multiplicative decomposition of the deformation gradient or the additive decomposition of the deformation rates are not used in the presented derivations. However, to visualize the quantity like $F^{\mathrm{el}} = F F_{\mathrm{d}}^{-1}$ one may use the notion of an intermediate or relaxed configuration. For discussions related to controversial meanings of such configurations in the case of general three-dimensional deformation we refer to Bertram (2012), Naghdi (1990), Xiao et al. (2006), among others.

As an example let us consider an elastic-non-linear-viscous material behavior under isothermal loading conditions. To simplify the model assume that the elastic strain is small $(\varepsilon^{\mathrm{el}})^2 \ll \varepsilon^{\mathrm{el}} < 1$. Small elastic strains are usually observed for metals. Furthermore assume that the inelastic deformation does not produce a significant change in volume such that

$$J = J^{\mathrm{el}} = (1 + \varepsilon^{\mathrm{el}})(1 - \nu\varepsilon^{\mathrm{el}})^2 \approx 1 + (1 - 2\nu)\varepsilon^{\mathrm{el}}, \quad \sigma J \approx \sigma, \tag{3.4.51}$$

where ν is the Poisson ratio. The constitutive equation for the stress has the following form[2]

$$\sigma = \frac{\partial \rho_0 \Phi(\varepsilon_{\mathrm{H}}^{\mathrm{el}})}{\partial \varepsilon_{\mathrm{H}}^{\mathrm{el}}} = \frac{\partial \rho_0 \Phi(\varepsilon_{\mathrm{H}} - \varepsilon_{\mathrm{H}}^{\mathrm{pl}})}{\partial(\varepsilon_{\mathrm{H}} - \varepsilon_{\mathrm{H}}^{\mathrm{pl}})} = E(\varepsilon_{\mathrm{H}} - \varepsilon_{\mathrm{H}}^{\mathrm{pl}}) \tag{3.4.52}$$

For the inelastic strain rate let us apply the power law type constitutive equation, as discussed in Sect. 3.2

$$\dot{\varepsilon}_{\mathrm{H}}^{\mathrm{pl}} = \dot{\varepsilon}_0 \left(\frac{|\sigma|}{\sigma_0} \right)^n \mathrm{sgn}(\sigma) \tag{3.4.53}$$

[2]The linear thermal expansion is neglected for the sake of brevity.

Assume that the rod is fixed at the cross section $X = 0$, i.e. $x(0, t) = 0$, and loaded at $x = \ell$ by the force $\mathcal{F}(t)$. Furthermore assume that the load is quasi-static such that the balance of momentum (2.3.25) can be reduced to the balance of internal force providing $\sigma(x, t)A(t) = \mathcal{F}(t)$. First let us subject the rod to the time-dependent elongation (strain-controlled test) such that

$$\varepsilon_{\mathrm{H}}(t) = \ln \frac{\ell(t)}{\ell_0} = \dot{\varepsilon}_{\mathrm{H}_0} t, \tag{3.4.54}$$

where $\dot{\varepsilon}_{\mathrm{H}_0}$ is a given constant strain rate. Let us compute the stresses $\sigma(x, t)$ and $P(x, t)$. To this end take the time derivative of Eq. (3.4.52) and apply the constitutive equation (3.4.53) to eliminate the inelastic strain rate. As a result the following differential equation for the stress σ can be derived

$$\dot{\sigma} + E\dot{\varepsilon}_0 \left(\frac{|\sigma|}{\sigma_0} \right)^n \operatorname{sgn}(\sigma) = E\dot{\varepsilon}_{\mathrm{H}} \tag{3.4.55}$$

For the loading defined by Eq. (3.4.54) the Eq. (3.4.55) can be put into the following normalized form

$$\frac{\mathrm{d}\Sigma}{\mathrm{d}\epsilon} + \frac{1}{\gamma}(\Sigma)^n = 1, \quad \Sigma = \frac{\sigma}{\sigma_0}, \quad \epsilon = \frac{E}{\sigma_0}\varepsilon_{\mathrm{H}}, \quad \gamma = \frac{\dot{\varepsilon}_{\mathrm{H}_0}}{\dot{\varepsilon}_0} \tag{3.4.56}$$

Equation (3.4.56) can be solved numerically with the initial condition $\Sigma(0) = 0$ providing the stress-strain curve. Figure 3.1a illustrates the results of the numerical integration for $n = 3$ and three different strain rates. The strain rate sensitivity of the inelastic range can be clearly observed. The flow stress in the steady state regime can be computed from Eq. (3.4.56) as follows

$$\frac{\mathrm{d}\Sigma}{\mathrm{d}\epsilon} = 0 \quad \Rightarrow \quad \Sigma_{\mathrm{ss}} = \gamma^{\frac{1}{n}}$$

or

$$\sigma_{\mathrm{ss}} = \sigma_0 \left(\frac{\dot{\varepsilon}_{\mathrm{H}_0}}{\dot{\varepsilon}_0} \right)^{\frac{1}{n}} \tag{3.4.57}$$

Equation (3.4.57) can be used to identify the material properties $\dot{\varepsilon}_0$, σ_0 and n from stress-strain diagrams. Once the true stress σ is given the engineering stress P can be computed with Eqs. (2.6.55) and (3.4.51) as follows

$$P = \sigma F^{-1} = \sigma \exp\left(-\frac{\sigma_0}{E}\epsilon \right)$$

Furthermore the engineering strain defined by Eq. (2.1.5) can be related to the true strain as follows

$$\varepsilon = 1 - \exp(\varepsilon_{\mathrm{H}})$$

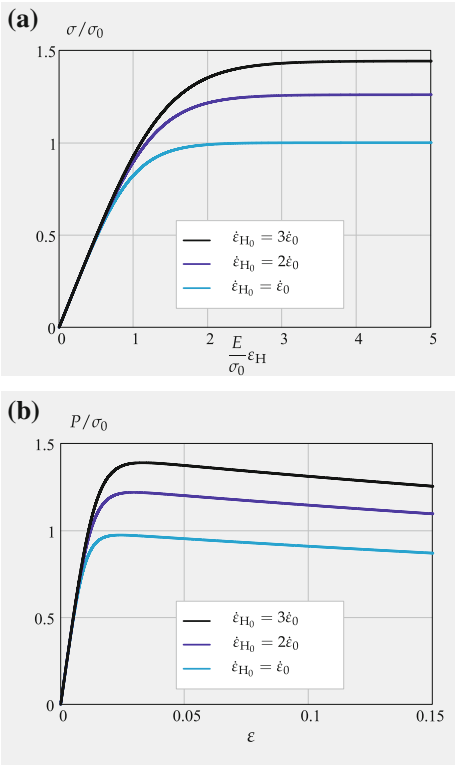

Fig. 3.1 Strain rate sensitivity of stress-strain diagrams for $n = 3$ and $E/\sigma_0 = 10$. **a** Normalized true stress versus normalized true strain. **b** Normalized engineering stress versus normalized engineering strain

Figure 3.1b shows the engineering stress as a function of the engineering strain for $E/\sigma_0 = 10$ and different strain rates. The engineering stress-strain curve exhibits a descending branch as a result of the cross section shrinkage. Note, that we assumed uniform elongation and consequently uniform cross section change. For the analysis of strain localization and necking instability the cross section shrinkage and its gradient are required as additional degrees of freedom, e.g. Antman (1973), Coleman (1986).

Besides the strain rate sensitivity the exponent n controls the transition from the elastic to the inelastic regime. To discuss this Fig. 3.2 shows the true stress-strain curves for the strain rate $\dot{\varepsilon}_H = \dot{\varepsilon}_0$ and different values of n. With an increase of n the curves approach the elastic-ideal plastic rate-independent regime.

In the next example assume that the rod is subjected to the constant tensile force $\mathcal{F}$. The rate of strain follows from Eq. (3.4.55)

$$\dot{\varepsilon}_H \left(1 - \frac{P}{E}\exp(\varepsilon_H)\right) = \dot{\varepsilon}_0 \left(\frac{P}{\sigma_0}\right)^n \exp\left(n\varepsilon_H\right), \quad P = \frac{\mathcal{F}}{A_0} \tag{3.4.58}$$

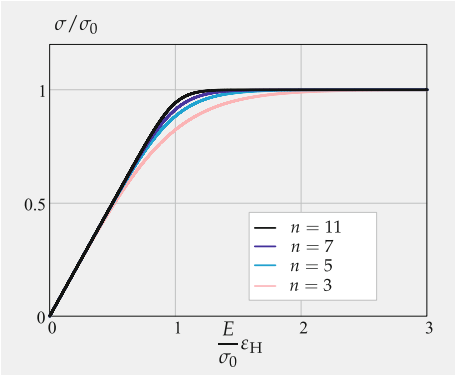

Fig. 3.2 Normalized true stress versus normalized true strain for the constant strain rate $\dot{\varepsilon}_H = \dot{\varepsilon}_0$ and different values of the exponent n

Equation (3.4.55) can be solved in a closed analytical form providing the relation between the strain and the time. To simplify this relation assume that

$$\frac{P}{E}\exp(\varepsilon_{H_{max}}) \ll 1$$

This can be well satisfied if the initial elastic strain after the loading is small, i.e. $P/E \ll 1$ and the maximum creep strain (strain before creep fracture) is $\varepsilon_{H_{max}} < 1$. In this case Eq. (3.4.55) takes the form

$$\dot{\varepsilon}_H = \dot{\varepsilon}_0 \left(\frac{P}{\sigma_0}\right)^n \exp\left(n\varepsilon_H\right) \tag{3.4.59}$$

The solution of Eq. (3.4.59) can be presented as follows

$$\varepsilon_H(t) = \varepsilon_H^{el} + \varepsilon_H^{pl}, \qquad \varepsilon_H^{pl} = -\frac{1}{n}\ln\left(1 - \frac{t}{t_*}\right), \quad t_* = \frac{1}{\dot{\varepsilon}_0 n}\left(\frac{\sigma_0}{P}\right)^n, \tag{3.4.60}$$

where ε_H^{el} is the initial elastic strain and t_* is the Hoff's time to ductile creep rupture (Hoff 1953). Figure 3.3 illustrates the creep curves according to Eqs. (3.4.60) for different values of the stress exponent. The introduced elasto-(visco)plastic model can capture the secondary creep stage and the tertiary creep stage due to the cross section shrinkage. Having a family of experimental creep curves for several stress levels one may identify the material properties $\dot{\varepsilon}_0$, σ_0 and n from creep curves. The value of σ_0 can be set arbitrarily, so that only two material constants in the power law creep are independent. Let us note that the power law creep is observed for narrow stress range. To capture creep behavior in a wide stress range advanced functions of stress are required (Altenbach et al. 2008b; Boyle 2012; Hosseini et al. 2013; Naumenko et al. 2009). Cross section shrinkage and the resulting tertiary creep were frequently observed in metals and alloys, for example Dünnwald and

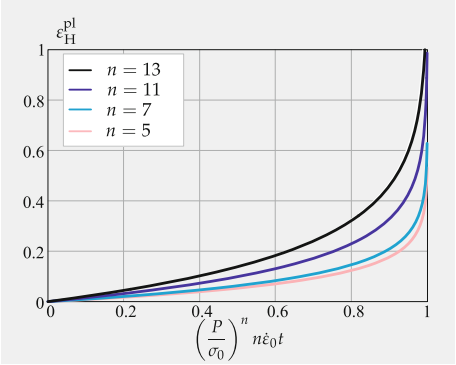

Fig. 3.3 Inelastic true strain versus normalized time for the constant force and different values of the exponent n

El-Magd (1996), El-Magd and Kranz (2000), Längler et al. (2014), Naumenko and Kostenko (2009). However, tertiary creep in metals and alloys may be controlled by additional material deterioration processes, see Sect. 1.2.1.2. Therefore Eq. (3.4.60) should be supplemented by additional kinetic equations to reflect softening, ageing and damage processes.

3.5 Hardening, Softening, and Ageing

Let us analyze several hardening mechanisms and present approaches to model macroscopic hardening phenomena. For the sake of brevity let us assume small strains such that the difference between true and engineering strain and stress measures is not essential and the geometrically-linear theory can be applied.

3.5.1 Strain Hardening

Inelastic flow of metals and alloys is accompanied by several hardening processes. An example is the dislocation generation as a result of inelastic strain accumulation. With the increase in dislocation density, the dislocation movement becomes more difficult such that the inelastic deformation rate decreases. At high temperature hardening effects may be reversed by annihilation processes that reduce the dislocation density. Therefore, the inelastic strain rate does not decrease towards zero, but attains a certain minimum or in some cases saturation value, see Sect. 1.1.1. A simple empirical approach is to introduce a strain hardening function h and to generalize a constitutive equation, for example a power law (3.4.53), as follows

$$\dot{\varepsilon}^{\mathrm{pl}} = \dot{\varepsilon}_0 \left(\frac{|\sigma|}{\sigma_0} \right)^n \mathrm{sgn}(\sigma) h(\varepsilon^{\mathrm{pl}}) \tag{3.5.61}$$

A popular choice for h is a power function

$$h(\varepsilon^{\mathrm{pl}}) = |\varepsilon^{\mathrm{pl}}|^l,$$

where the power l, $-1 < l < 0$ has to be identified from experimental data. Limitations of the empirical approach will be discussed in Sect. 5.3.1. Alternatively, hardening can be considered as a process and described by an independent rate-type equation. In the materials science a mean dislocation density variable ϱ is introduced to capture a hardening state of the material. Following Estrin (1996) the power law (3.4.53) can be generalized as follows

$$\dot{\varepsilon}^{\mathrm{pl}} = \dot{\varepsilon}_0 \left(\frac{|\sigma|}{\hat{\sigma}} \right)^n \mathrm{sgn}\sigma, \tag{3.5.62}$$

where $\hat{\sigma}$ is called drag stress and defined as follows

$$\hat{\sigma} = MGb\sqrt{\varrho}, \tag{3.5.63}$$

where M is the Taylor factor and b is the magnitude of the Burgers vector. Equation (3.5.63) assumes a simple, linear relationship between the drag stress and the dislocation density. As the latter increases in the course of inelastic deformation, the strain rate decreases, according to Eq. (3.5.62). In the continuum mechanics variables like mean dislocation density do not appear in the balance equations, and are not introduced at the beginning together with displacement, strain, density and others. However, as the dislocation density variable affects the inelastic strain rate and the stress, one may apply a concept of internal state or hidden state variables as proposed by Coleman and Gurtin (1967).[3] To explain this concept let us introduce a dimensionless hardening parameter

$$H = \sqrt{\frac{\varrho}{\varrho_0}}, \tag{3.5.64}$$

where ϱ_0 is a reference dislocation density. The constitutive equation (3.5.62) takes the form

$$\dot{\varepsilon}^{\mathrm{pl}} = \dot{\varepsilon}_0 \left(\frac{|\sigma|}{\sigma_0 H} \right)^n \mathrm{sgn}\sigma, \quad \sigma_0 = MGb\sqrt{\varrho_0} \tag{3.5.65}$$

[3] A historical essay on the development of theories with internal state variables is presented in Maugin (2015).

Under the assumption of small strains the inequality (2.6.50) takes the following form

$$\sigma\dot{\varepsilon} - \rho\dot{\Phi} - \rho\mathcal{S}\dot{T} - q\frac{T'}{T} \geq 0 \tag{3.5.66}$$

Let us postulate the following split of the mechanical power

$$\begin{aligned} \mathcal{L} &= \sigma\dot{\varepsilon} = \mathcal{L}_\mathrm{s} + \mathcal{L}_\mathrm{d}, \\ \mathcal{L}_\mathrm{s} &= \sigma_\mathrm{s}(\varepsilon^\mathrm{el}, T)\dot{\varepsilon}^\mathrm{el}, \\ \mathcal{L}_\mathrm{d} &= \sigma_\mathrm{d}(\dot{\varepsilon}^\mathrm{pl}, H, T)\dot{\varepsilon}^\mathrm{pl} \end{aligned} \tag{3.5.67}$$

According to (3.5.67) the stored part is a function of the elastic strain and the temperature, while the dissipated part involves the new variable H to capture the influence of hardening on the inelastic process. As in the Sect. 3.5 let us use the iso-stress approach such that

$$\sigma = \sigma_\mathrm{s}(\varepsilon^\mathrm{el}, T) = \sigma_\mathrm{d}(\dot{\varepsilon}^\mathrm{pl}, H, T)$$

Furthermore, assume that the free energy now is a function of the elastic strain, the hardening and the temperature. The inequality (3.5.66) takes the form

$$\left(\sigma - \rho\frac{\partial\Phi}{\partial\varepsilon^\mathrm{el}}\right)\dot{\varepsilon}^\mathrm{el} - \rho\left(\frac{\partial\Phi}{\partial T} + \mathcal{S}\right)\dot{T} + \sigma\dot{\varepsilon}^\mathrm{pl} - \rho\frac{\partial\Phi}{\partial H}\dot{H} - q\frac{T'}{T} \geq 0 \tag{3.5.68}$$

To resolve the inequality assume that the internal state variable H is defined by the following evolution equation

$$\dot{H} = f_H(\varepsilon^\mathrm{el}, T, H, \dot{\varepsilon}^\mathrm{pl}) \tag{3.5.69}$$

Then, for $\dot{\varepsilon}^\mathrm{el}$ and $\dot{T}$ that can be positive or negative the inequality is satisfied for

$$\sigma = \rho\frac{\partial\Phi}{\partial\varepsilon^\mathrm{el}}, \quad \mathcal{S} = -\frac{\partial\Phi}{\partial T}, \quad -q\frac{T'}{T} \geq 0, \quad \sigma\dot{\varepsilon}^\mathrm{pl} - \rho\frac{\partial\Phi}{\partial H}\dot{H} \geq 0 \tag{3.5.70}$$

The last inequality provides a restriction on the material properties and/oder response functions that enter the model. As an example let us assume that the hardening part of the free energy is proportional to $(H_\infty - H)^2$, where H_∞ is the saturation value of the hardening variable, which may depend on the stress or minimum inelastic strain rate. Then

$$-\rho\frac{\partial\Phi}{\partial H} = A_\mathrm{h}(H_\infty - H), \tag{3.5.71}$$

where Ah is a positive constant. For the hardening rate let us apply the following equation

$$\dot{H} = B\,(H_\infty - H)\,|\dot{\varepsilon}^{\mathrm{pl}}|, \tag{3.5.72}$$

where B is a positive constant. Equation (3.5.72) assumes that the "driving force" for the hardening process is $(H_\infty - H)$, as given by Eq. (3.5.71), and that the kinetics of hardening is related to the inelastic strain rate magnitude. Equations like (3.5.71) are applied in Estrin (1996), Blum (2008), Naumenko and Gariboldi (2014), among others, for modeling hardening in several alloys. With the constitutive equations (3.5.62) and (3.5.71) as well as the evolution equation (3.5.71) we obtain

$$\sigma\,\dot{\varepsilon}^{\mathrm{pl}} - \rho\frac{\partial \Phi}{\partial H}\dot{H} = \left[|\sigma| + A_{\mathrm{h}} B\,(H_\infty - H)^2\right]|\dot{\varepsilon}^{\mathrm{pl}}| \geq 0 \tag{3.5.73}$$

With the proposed constitutive Eq. (3.5.71) and evolution Eq. (3.5.72) the inequality (3.5.73) is satisfied.

As an example consider a small strain creep regime with $\sigma = \mathrm{const} > 0$. For the constant stress Eq. (3.5.72) can be integrated providing the hardening variable as a function of the inelastic strain. As a result we obtain

$$H = H_\infty - (H_\infty - 1)\exp\left(-B\varepsilon^{\mathrm{pl}}\right) \tag{3.5.74}$$

After inserting in the constitutive equation (3.5.65) we obtain

$$\dot{\varepsilon}^{\mathrm{pl}} = \dot{\varepsilon}_0 \left(\frac{\sigma}{\sigma_0 H_\infty}\right)^n \left[1 - \left(1 - \frac{1}{H_\infty}\right)\exp\left(-B\varepsilon^{\mathrm{pl}}\right)\right]^{-n} \tag{3.5.75}$$

Obviously, for the constant stress the model with the internal state variable provides the creep model with the exponential type strain hardening function. The material properties can be identified from a family of creep curves. As H_∞ is a function of stress, it is not possible to solve Eq. (3.5.72) in terms of elementary functions for other cases of loading, for example for the tensile regime. Standard numerical solution techniques for ordinary differential equations can be applied for the solution in a general case of loading.

Let us go back to the mean dislocation density model. With Eq. (3.5.64) the evolution equation (3.5.72) takes the following form

$$\dot{\varrho} = \left(k_1\sqrt{\varrho} - k_2\varrho\right)|\dot{\varepsilon}^{\mathrm{pl}}|, \quad k_1 = 2B\sqrt{\varrho_\infty}, \quad k_2 = 2B \tag{3.5.76}$$

Similar equation is derived in Estrin (1996), where the term $k_1\sqrt{\varrho}$ is associated with the storage of dislocations and $k_2\varrho$—with recovery of dislocations.

3.5.2 Kinematic Hardening

Another mechanism of hardening can be related to the micro-stress fields generated during the plastic flow, as a result of heterogeneous deformation on the micro-scale. Several microstructural zones, for example slip planes, grains with certain crystallographic orientations or certain regions within subgrains may exhibit higher levels of inelastic strain rate. The remaining part of microstructure behaves more or less elastically. This leads to changes of micro-stress states and to formation of residual stresses upon unloading. Residual micro-stress fields affect the overall deformation rate and provide an additional hardening.

To derive a robust phenomenological model by taking into account micro-stress fields consider again the following split of the mechanical power[4]

$$\mathcal{L} = \sigma\dot{\varepsilon} = \sigma\dot{\varepsilon}^{\mathrm{el}} + \sigma\dot{\varepsilon}^{\mathrm{pl}}$$

Now assume that a part of the mechanical power $\sigma\dot{\varepsilon}^{\mathrm{pl}}$ is stored in the course of inelastic deformation. To this end let us consider the following decomposition

$$\sigma = \sigma_{\mathrm{a}} + \beta, \quad \varepsilon^{\mathrm{pl}} = \varepsilon^{\mathrm{rec}} + \varepsilon^{\mathrm{pm}}, \quad \sigma\dot{\varepsilon}^{\mathrm{pl}} = \sigma_{\mathrm{a}}\dot{\varepsilon}^{\mathrm{pl}} + \beta\dot{\varepsilon}^{\mathrm{rec}} + \beta\dot{\varepsilon}^{\mathrm{pm}}, \tag{3.5.77}$$

where σ_{a} is the active stress and β is the backstress. $\varepsilon^{\mathrm{rec}}$ is the recoverable inelastic strain while $\varepsilon^{\mathrm{pm}}$ is the permanent inelastic strain. These strain components are illustrated in Fig. 1.11b. Now define the quasi-conservative and dissipated parts of the mechanical power as follows

$$\begin{aligned} \mathcal{L}_{\mathrm{s}} &= \sigma(\varepsilon^{\mathrm{el}}, T)\dot{\varepsilon}^{\mathrm{el}} + \beta(\varepsilon^{\mathrm{rec}}, T)\dot{\varepsilon}^{\mathrm{rec}}, \\ \mathcal{L}_{\mathrm{d}} &= \sigma_{\mathrm{a}}(\dot{\varepsilon}^{\mathrm{pl}}, T)\dot{\varepsilon}^{\mathrm{pl}} + \beta(\dot{\varepsilon}^{\mathrm{pm}}, T)\dot{\varepsilon}^{\mathrm{pm}} \end{aligned} \tag{3.5.78}$$

Furthermore assume that the free energy depends on the elastic strain, the recoverable inelastic strain and the temperature. With these assumptions the inequality (3.5.66) takes the form

$$\begin{aligned} \left(\sigma - \rho\frac{\partial\Phi}{\partial\varepsilon^{\mathrm{el}}}\right)\dot{\varepsilon}^{\mathrm{el}} + \left(\beta - \rho\frac{\partial\Phi}{\partial\varepsilon^{\mathrm{rec}}}\right)\dot{\varepsilon}^{\mathrm{rec}} - \rho\left(\frac{\partial\Phi}{\partial T} + \mathcal{S}\right)\dot{T} \\ +\sigma_{\mathrm{a}}\dot{\varepsilon}^{\mathrm{pl}} + \beta\dot{\varepsilon}^{\mathrm{pm}} - q\frac{T'}{T} \geq 0 \end{aligned} \tag{3.5.79}$$

The first line in (3.5.79) is a linear function of three independent rates $\dot{\varepsilon}^{\mathrm{el}}$, $\dot{\varepsilon}^{\mathrm{rec}}$ and T. Since these rates may be positive or negative, the inequality (3.5.79) can be resolved as follows

$$\begin{aligned} \sigma = \rho\frac{\partial\Phi}{\partial\varepsilon^{\mathrm{el}}}, \quad \beta = \rho\frac{\partial\Phi}{\partial\varepsilon^{\mathrm{rec}}}, \quad \mathcal{S} = -\frac{\partial\Phi}{\partial T}, \\ -q\frac{T'}{T} \geq 0, \quad \sigma_{\mathrm{a}}\dot{\varepsilon}^{\mathrm{pl}} + \beta\dot{\varepsilon}^{\mathrm{pm}} \geq 0 \end{aligned} \tag{3.5.80}$$

[4]Here we assume again small strains for the sake of brevity.

For the stress and the backstress let us assume the following constitutive equations

$$\sigma = \rho \frac{\partial \Phi}{\partial \varepsilon^{\mathrm{el}}} = E\varepsilon^{el}, \quad \beta = \rho \frac{\partial \Phi}{\partial \varepsilon^{\mathrm{rec}}} = E_{\mathrm{h}}\varepsilon^{\mathrm{rec}}, \tag{3.5.81}$$

where E_{h} is the temperature-dependent hardening modulus. For the rate of the plastic strain let us apply Eq. (3.4.50) with respect to the active part of the stress

$$\dot{\varepsilon}^{\mathrm{pl}} = f_\sigma(|\sigma_{\mathrm{a}}|)\mathrm{sgn}(\sigma_{\mathrm{a}})f_T(T) = f_\sigma(|\sigma - \beta|)\mathrm{sgn}(\sigma - \beta)f_T(T), \tag{3.5.82}$$

For the rate of the permanent strain let us apply the following equation

$$\dot{\varepsilon}^{\mathrm{pm}} = g_\sigma(|\beta|)\mathrm{sgn}(\beta)g_T(T) \tag{3.5.83}$$

For f_σ and g_σ one may apply, for example, power law functions. For $f_T(T)$ and $g_T(T)$ Arrhenius type functions of temperature can be used. Response functions of stress and temperature will be discussed in Sect. 5.4.4. Alternatively, one may assume that the rate of the permanent strain is related to the rate of plastic strain and the backstress as follows

$$\dot{\varepsilon}^{\mathrm{pm}} = \frac{\beta}{\beta_*}|\dot{\varepsilon}^{\mathrm{pl}}|, \tag{3.5.84}$$

where β_* can be a function of stress and temperature. One may verify that with Eqs. (3.5.82) and (3.5.83) or (3.5.84) the last inequality in (3.5.80) is satisfied. Let us derive the rate equation for the backstress. To this end take the time derivative of the constitutive equation $(3.5.81)_2$

$$\dot{\beta} = \frac{\mathrm{d}E_{\mathrm{h}}}{\mathrm{d}T}\dot{T}\varepsilon^{\mathrm{rec}} + E_{\mathrm{h}}\dot{\varepsilon}^{\mathrm{rec}} = \frac{1}{E_{\mathrm{h}}}\frac{\mathrm{d}E_{\mathrm{h}}}{\mathrm{d}T}\beta\dot{T} + E_{\mathrm{h}}(\dot{\varepsilon}^{\mathrm{pl}} - \dot{\varepsilon}^{\mathrm{pm}}) \tag{3.5.85}$$

With the Eq. (3.5.83) we obtain

$$\dot{\beta} = \frac{1}{E_{\mathrm{h}}}\frac{\mathrm{d}E_{\mathrm{h}}}{\mathrm{d}T}\beta\dot{T} + E_{\mathrm{h}}[\dot{\varepsilon}^{\mathrm{pl}} - g_\sigma(|\beta|)\mathrm{sgn}(\beta)g_T(T)] \tag{3.5.86}$$

Assuming isothermal loading conditions $\dot{T} = 0$, Eq. (3.5.86) simplifies to

$$\dot{\beta} = E_{\mathrm{h}}[\dot{\varepsilon}^{\mathrm{pl}} - g_\sigma(|\beta|)\mathrm{sgn}(\beta)g_T(T)] \tag{3.5.87}$$

Equation (3.5.87) was postulated by Malinin and Khadjinsky (1972) without the analysis of the thermodynamic process and splitting the mechanical power. The constitutive equation (3.5.82) and the evolution equation (3.5.87) is an example of the hardening model with the backstress. As shown in Malinin and Khadjinsky (1972) such a model can describe various effects of inelastic deformation including creep recovery, cyclic hardening, etc. A more detailed analysis will be given in Sect. 5.3.2.

Applying the constitutive assumption (3.5.84) and with Eq. (3.5.85) we obtain

$$\dot{\beta} = \frac{1}{E_\mathrm{h}} \frac{dE_\mathrm{h}}{dT} \beta \dot{T} + E_\mathrm{h} \left(\dot{\varepsilon}^\mathrm{pl} - \frac{\beta}{\beta_*} |\dot{\varepsilon}^\mathrm{pl}| \right) \tag{3.5.88}$$

For isothermal loading conditions this simplifies to

$$\dot{\beta} = E_\mathrm{h} \left(\dot{\varepsilon}^\mathrm{pl} - \frac{\beta}{\beta_*} |\dot{\varepsilon}^\mathrm{pl}| \right) \tag{3.5.89}$$

Equation (3.5.89) was proposed by Frederick and Armstrong (2007).[5] It is obvious, that different versions for a model with a backstress can be obtained by specifying the constitutive equation for the rate of permanent inelastic strain. A simplest version can be obtained assuming

$$\beta = E_\mathrm{h} \varepsilon^\mathrm{pl}$$

This linear hardening rule was proposed by Prager (1956). Instead the constitutive equation (3.4.50) one may use a rate-independent plasticity model of the type (3.3.36). The yield condition is then formulated with respect to the active stress i.e.

$$|\sigma - \beta| - \sigma_\mathrm{y} = 0$$

For the given accumulated value of the backstress the actual yield condition is shifted or translated if compared to the original one with the zero backstress. Therefore this approach was called kinematic hardening. For different versions of the kinematic hardening rules we refer to Chaboche (1989, 2008), Lemaitre and Chaboche (1990), Lemaitre et al. (2009).

Let us analyze the constitutive equation for the plastic strain rate (3.5.82) and the evolution equation (3.5.89) for different loading cases. To this end let us specify the constitutive Eq. (3.5.82) assuming a power function of stress

$$\dot{\varepsilon}^\mathrm{pl} = \dot{\varepsilon}_0 \left(\frac{|\sigma - \beta|}{\sigma_0} \right)^n \mathrm{sgn}(\sigma - \beta), \tag{3.5.90}$$

where $\dot{\varepsilon}_0, \sigma_0$ and n are material properties. First consider a creep regime for the constant tensile stress. In this case the evolution equation (3.5.89) can be integrated in elementary functions. With the initial condition $\beta(0) = 0$ the result is

$$\beta = \beta_* \left[1 - \exp\left(-\frac{E_\mathrm{h}}{\beta_*} \varepsilon^\mathrm{pl} \right) \right] \tag{3.5.91}$$

[5] The model was firs published in 1966 in a CEGB report, see Frederick and Armstrong (2007) for historical remarks.

With (3.5.90) the following expression for the inelastic strain rate can be obtained

$$\dot{\varepsilon}^{\mathrm{pl}} = \dot{\varepsilon}_0 \left(\frac{\sigma}{\sigma_0}\right)^n \left[1 - \frac{\beta_*}{\sigma} + \frac{\beta_*}{\sigma} \exp\left(-\frac{E_{\mathrm{h}}}{\beta_*}\varepsilon^{\mathrm{pl}}\right)\right]^n \tag{3.5.92}$$

Equation (3.5.92) describes the primary stage of the creep curve. It is obvious that for the loading with constant stress the exponential type strain hardening function follows from the backstress model. The material parameters and the function β_* in Eq. (3.5.92) can be identified from a family of creep curves considering the primary creep stage.

To simulate strain and/or stress responses under timely varying loading Eqs. (3.5.82) and (3.5.89) can be solved numerically. Let us introduce new variables: the normalized time $\tau = \dot{\varepsilon}_0 t$, the normalized stress $\Sigma = \sigma/\sigma_0$ and the following dimensionless constants

$$\tilde{E}_{\mathrm{h}} = \frac{\tilde{E}_{\mathrm{h}}}{\sigma_0}, \quad \tilde{E} = \frac{\tilde{E}}{\sigma_0}$$

Equations (3.5.82) and (3.5.89) take the following form

$$\begin{aligned} \frac{\mathrm{d}\varepsilon^{\mathrm{pl}}}{\mathrm{d}\tau} &= |\Sigma - \tilde{E}_{\mathrm{h}}\varepsilon^{\mathrm{rec}}|^n \mathrm{sgn}(\Sigma - \tilde{E}_{\mathrm{h}}\varepsilon^{\mathrm{rec}}), \\ \frac{\mathrm{d}\varepsilon^{\mathrm{rec}}}{\mathrm{d}\tau} &= \frac{\mathrm{d}\varepsilon^{\mathrm{pl}}}{\mathrm{d}\tau} - \frac{\varepsilon^{\mathrm{rec}}}{\varepsilon^{\mathrm{rec}}_*}\left|\frac{\mathrm{d}\varepsilon^{\mathrm{pl}}}{\mathrm{d}\tau}\right|, \end{aligned} \tag{3.5.93}$$

where

$$\varepsilon^{\mathrm{rec}}_* = \frac{\beta_*}{\tilde{E}_{\mathrm{h}}}\Sigma$$

For the simulations let us assume the following values

$$n = 3, \quad \tilde{E}_{\mathrm{h}} = 100, \quad \tilde{E} = 1000, \quad B_* = 0.9 \tag{3.5.94}$$

Figure 3.4a shows two normalized stress versus normalized time profiles. Here three loading steps are assumed as follows. During the first step the stress is kept constant over a period of time. Then the stress value is reduced to the half of the value in the first cycle and kept constant for the same period of time. After that the stress is increased up to the original value and kept constant. Figure 3.4b illustrates the corresponding creep strain versus time responses. The first loading step provides a typical primary creep regime. After the unloading a creep recovery during the second loading step is observed. The loading to the same stress value leads again to the primary creep regime with a decrease of the inelastic strain rate over the time. However, the starting creep rate after the second loading is lower that the corresponding creep rate at the beginning of the loading sequence.

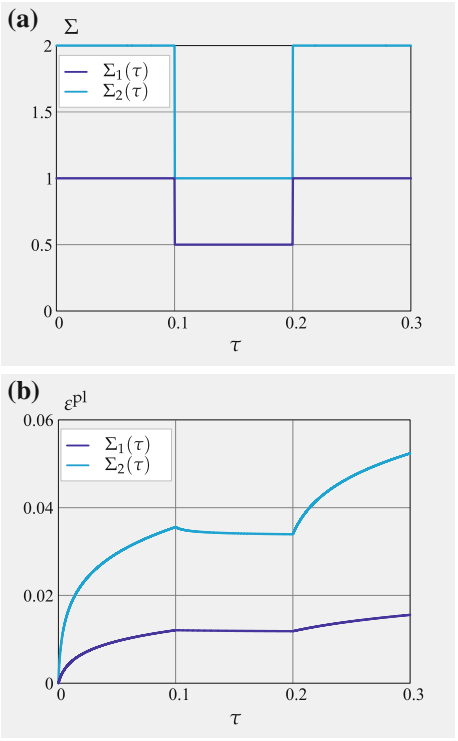

Fig. 3.4 Simulation of creep response under variable loading with Eqs. (3.5.93) and parameters (3.5.94). **a** Loading profiles. **b** Inelastic strain versus normalized time

Let us analyze stress responses under the strain control. Taking the time derivative of stress we obtain

$$\dot{\sigma} = E(\dot{\varepsilon} - \dot{\varepsilon}^{\mathrm{pl}})$$

With the introduced normalized variables this equation reads

$$\frac{\mathrm{d}\Sigma}{\mathrm{d}\tau} = \tilde{E}\left(\frac{\dot{\varepsilon}}{\dot{\varepsilon}_0} - \frac{\mathrm{d}\varepsilon^{\mathrm{pl}}}{\mathrm{d}\tau}\right) \tag{3.5.95}$$

For a given strain profile $\varepsilon(\tau)$, Eq. (3.5.95) can be integrated numerically together with Eqs. (3.5.93). Figure 3.5a shows two strain versus time profiles corresponding to LCF loading regimes. The stress-strain hysteresis loops are presented in Fig. 3.5b. We observe that the Frederick-Armstrong type kinematic hardening model is able to reproduce several phenomena observed in LCF tests. They include the Bauschinger effect: in the first loading cycle the absolute value of the apparent yield point under compression is lower than the corresponding value under tension, the cyclic hardening: the stress amplitude increases in the course of cyclic loading, and the strain rate sensitivity: the stress-strain loop depends on the rate of loading. The Frederick-

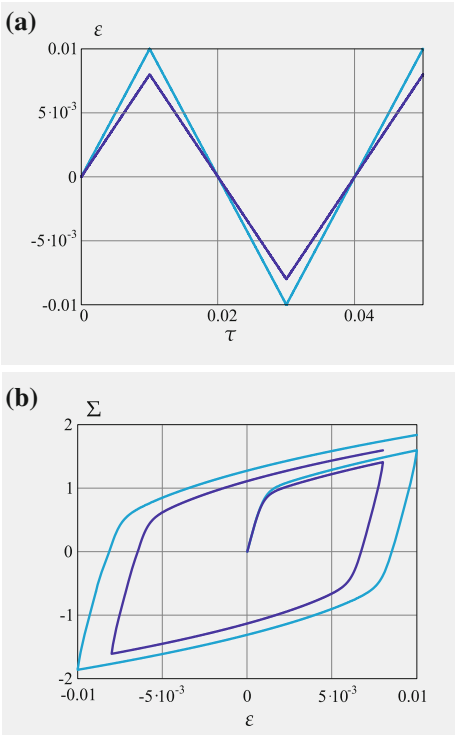

Fig. 3.5 Simulation of stress response under cyclic strain with Eq. (3.5.95) and parameters (3.5.94). **a** Loading profiles. **b** Normalized stress versus strain

Armstrong model was calibrated and applied to describe inelastic behavior of many materials. Examples are presented in Altenbach et al. (2013), Chaboche (2008), Längler et al. (2014), among others. In describing material behavior over many loading cycles modifications may be required. For example the model can lead to an overestimation of cyclic strain accumulation in the creep ratchetting regime (Altenbach et al. 2013; Ohno et al. 1998; Ohno 1998). As discussed in Ohno et al. (1998) the deficiency is primarily related to the constitutive assumption (3.5.84). Various modifications of the Frederick-Armstrong model to capture the material behavior under cyclic loading are discussed by Ohno et al. (1998).

3.5.3 Phase Mixture Models for Hardening and Softening

Many materials contain relatively high dislocation density at the initial (virgin) state after the processing. Examples include 9–12% Cr ferritic steels, where a high density of dislocations is induced after martensitic transformation. High dislocation density, fine subgrain structure and different types of precipitates are examples of microstructural features that improve creep strength and high-temperature resistance

Abe (2009), Dyson and McLean (1998), Blum (2008), Straub (1995). For these materials the inelastic deformation is accompanied by softening processes such as recovery of dislocation substructures and coarsening of subgrains (Blum 2008). Stress-strain curves of softening materials show descending (softening) branch, Fig. 1.2 and creep curves exhibit accelerated regime immediately after the primary creep stage, Fig. 1.9.

To characterize hardening and softening processes a phase mixture model (or composite model) can be applied. The basic idea is to idealize the heterogeneous inelastic deformation in a volume element by considering a mixture with two or more constituents with different, but homogeneous inelastic properties. Assuming the total deformation of constituents to be the same, redistribution of stresses would take place, leading to the decrease of the overall inelastic strain rate. For example, in Straub (1995), Polcik et al. (1998), Polcik (1999), Barkar and Ågren (2005) two phases are introduced including the inelastic hard phase for subgrain boundaries with a relatively high dislocation density and the inelastic soft one for subgrain interiors. Two different sets of constitutive equations for inelastic strains are formulated. Furthermore, the volume fraction of the hard constituent is assumed to decrease over time to capture the coarsening process.

Let us explain the phase mixture approach by assuming two constituents with different inelastic behavior. For the sake of brevity, let us assume that constituents have the same elastic properties. Furthermore, as in the previous subsections we assume small strains, to keep the derivations brief and transparent. To designate the properties of the constituents the subscripts s (for inelastic-soft) and h (for inelastic hard) will be used. Let ε_s and ε_h be the strains of the constituents and σ_s and σ_h the corresponding effective stresses. For the stress of the composite the following mixture rule can be applied

$$\sigma = (1 - \eta_\mathrm{h})\sigma_\mathrm{s} + \eta_\mathrm{h}\sigma_\mathrm{h} \tag{3.5.96}$$

where η_h is the volume fraction of the inelastic-hard constituent. With respect to the total strains let us postulate the following rule

$$\varepsilon = \varepsilon_\mathrm{h} = \varepsilon_\mathrm{s} \tag{3.5.97}$$

For the effective stress components the following constitutive equations can be assumed

$$\sigma_\mathrm{s} = E(\varepsilon - \varepsilon_\mathrm{s}^\mathrm{pl}), \qquad \sigma_\mathrm{h} = E(\varepsilon - \varepsilon_\mathrm{h}^\mathrm{pl}) \tag{3.5.98}$$

With Eq. (3.5.96) the stress of the mixture is computed as follows

$$\sigma = E(\varepsilon - \varepsilon^\mathrm{pl}), \qquad \varepsilon^\mathrm{pl} = (1 - \eta_\mathrm{h})\varepsilon_\mathrm{s}^\mathrm{pl} + \eta_\mathrm{h}\varepsilon_\mathrm{h}^\mathrm{pl} \tag{3.5.99}$$

For the inelastic strain rates one may assume the following constitutive equations

$$\dot{\varepsilon}_{\mathrm{s}}^{\mathrm{pl}} = f_{\mathrm{s}}(|\sigma_{\mathrm{s}}|)\mathrm{sgn}\sigma_{\mathrm{s}}, \qquad \dot{\varepsilon}_{\mathrm{h}}^{\mathrm{pl}} = f_{\mathrm{h}}(|\sigma_{\mathrm{h}}|)\mathrm{sgn}\sigma_{\mathrm{h}}, \tag{3.5.100}$$

where f_{s} and f_{h} are response functions of stress, for example power laws. Instead of Eq. (3.5.100) one may apply more advanced constitutive and evolution equations with dislocation type hardening or/and backstress as discussed in Sects. 3.5.1 and 3.5.2. Examples are presented in Straub (1995), Polcik et al. (1998), Polcik (1999), Barkar and Ågren (2005), Raj et al. (1996). Let us note that if the volume fractions are kept constant, then Eqs. (3.5.97)–(3.5.100) is nothing else as a connection of hard and soft elements in parallel, where both hard and soft elements is a series connection of an elastic spring and non-linear dashpots. Such connections in various combinations are discussed in rheology (Reiner 1969; Giesekus 1994; Palmov 1998). Rheological models, equipped with constant volume fractions were firstly applied in Besseling (1958), Besseling and van der Giessen (1994) to model inelastic material behavior and, in particular to motivate kinematic hardening rules. A more general approach is to introduce kinetic equations for the volume fractions. For example, assuming that the volume fraction of the hard constituent is decreasing over time, softening process associated with change of the microstructure can be described. In Straub (1995), Polcik et al. (1998), Polcik (1999), Barkar and Ågren (2005) the volume fraction η_{h} is related to the mean subgrain size. The increase in the subgrain size, or decrease of η_{h} is described with an exponential-type kinetic equation. It is calibrated against experimental data of substructure evolution based on in situ transmission electron microscope observations.

Equations (3.5.97)–(3.5.100) and a kinetic equation for the volume fraction can be used to simulate macroscopic material response for different types of loading. Such a simulation is feasible if material parameters in constitutive and evolution equations for constituents are well defined either from tests or from simulations at the microscale. An alternative approach is to reduce Eqs. (3.5.97)–(3.5.100) to obtain a macroscopic model with internal state variables. Then all response functions and material properties can be identified from macroscopic tests. As an example consider an approach presented in Naumenko et al. (2011a) to model hardening and softening in advanced steel. Instead of (3.5.100) the following constitutive equations are assumed

$$\dot{\varepsilon}_{\mathrm{s}}^{\mathrm{pl}} = f_{\mathrm{s}}(|\sigma_{\mathrm{s}}|)\mathrm{sgn}\sigma_{\mathrm{s}}, \qquad \dot{\varepsilon}_{\mathrm{h}}^{\mathrm{pl}} = \frac{\sigma_{\mathrm{h}} - \sigma}{\sigma_{\mathrm{h}_*} - \sigma}|\dot{\varepsilon}^{\mathrm{pl}}|, \tag{3.5.101}$$

where σ_{h_*} is the saturation stress in the hard constituent. In Eqs. (3.5.101) the inelastic part of the soft constituent is determined by the non-linear viscosity function f_{s}. The inelastic strain rate of the hard constituent is proportional to the magnitude of the overall creep rate and the overstress $\sigma_{\mathrm{ov}} = \sigma_{\mathrm{h}} - \sigma$. As the elastic properties of constituents are assumed the same, after the loading in elastic range $\sigma_{\mathrm{h}} = \sigma, \sigma_{\mathrm{ov}} = 0$

and the inelastic strain rate of the hard constituent is zero. When $\sigma_{\mathrm{h}} \to \sigma_{\mathrm{h}_*}$, where σ_{h_*} is the saturation stress, the inelastic strain rate of the hard constituent in tensile regime approaches to the inelastic strain rate of the composite. Then $\dot{\varepsilon}_{\mathrm{s}}^{\mathrm{pl}} = \dot{\varepsilon}_{\mathrm{h}}^{\mathrm{pl}}$ and the stresses in both constituents approach the asymptotic values. For the sake of brevity let us assume isothermal loading. Taking the time derivative of Eq. (3.5.98) and applying Eq. (3.5.101) we obtain

$$\dot{\varepsilon}_{\mathrm{s}} = \frac{\dot{\sigma}_{\mathrm{s}}}{E} + f(|\sigma_{\mathrm{s}}|)\mathrm{sgn}\sigma_{\mathrm{s}}, \qquad \dot{\varepsilon}_{\mathrm{h}} = \frac{\dot{\sigma}_{\mathrm{h}}}{E} + \frac{\sigma_{\mathrm{h}} - \sigma}{\sigma_{\mathrm{h}_*} - \sigma}|\dot{\varepsilon}^{\mathrm{pl}}| \tag{3.5.102}$$

The strain rate of the mixture can be computed applying Eq. $(3.5.99)_1$ as follows

$$\dot{\varepsilon} = \frac{\dot{\sigma}}{E} + \dot{\varepsilon}^{\mathrm{pl}} \tag{3.5.103}$$

For the identification it is convenient to introduce the following new variables

$$\begin{aligned}
&\beta = \frac{\eta_{\mathrm{h}_0}}{1-\eta_{\mathrm{h}_0}}(\sigma_{\mathrm{h}} - \sigma), \quad 0 \le \beta \le \beta_*, \quad \beta_* = \frac{\eta_{\mathrm{h}_0}}{1-\eta_{\mathrm{h}_0}}(\sigma_{\mathrm{h}_*} - \sigma),\\
&\Gamma = \frac{\eta_{\mathrm{h}}}{1-\eta_{\mathrm{h}}}\frac{1-\eta_{\mathrm{h}_0}}{\eta_{\mathrm{h}_0}}, \quad \Gamma_* \le \Gamma \le 1, \quad \Gamma_* = \frac{\eta_{\mathrm{h}_*}}{1-\eta_{\mathrm{h}_*}}\frac{1-\eta_{\mathrm{h}_0}}{\eta_{\mathrm{h}_0}},
\end{aligned}$$

where η_{h_0} is the reference value of η_{h}. Equations (3.5.97)–(3.5.100) and (3.5.101)–(3.5.103) can be transformed to

$$\begin{aligned}
&\dot{\varepsilon}^{\mathrm{pl}} = f(|\sigma - \beta\Gamma|)\frac{\sigma - \beta\Gamma}{|\sigma - \beta\Gamma|} - \frac{1}{E}\frac{\mathrm{d}}{\mathrm{d}t}(\beta\Gamma),\\
&\dot{\beta} = \frac{E}{c_{\mathrm{h}}}\left(\dot{\varepsilon}^{\mathrm{pl}} - |\dot{\varepsilon}^{\mathrm{pl}}|\frac{\beta}{\beta_*}\right), \quad c_{\mathrm{h}} = \frac{1-\eta_{\mathrm{h}_0}}{\eta_{\mathrm{h}_0}}
\end{aligned} \tag{3.5.104}$$

In Eq. (3.5.104) β and Γ play now the role of internal state variables. If the fraction is kept constant then by setting $\Gamma = 1$ we obtain

$$\begin{aligned}
&\dot{\varepsilon}^{\mathrm{pl}} = f(|\sigma - \beta|)\frac{\sigma - \beta}{|\sigma - \beta|} - \underline{\frac{1}{E}\frac{\mathrm{d}}{\mathrm{d}t}(\beta)},\\
&\dot{\beta} = \frac{E}{c_{\mathrm{h}}}\left(\dot{\varepsilon}^{\mathrm{pl}} - |\dot{\varepsilon}^{\mathrm{pl}}|\frac{\beta}{\beta_*}\right)
\end{aligned} \tag{3.5.105}$$

The underlined term influences the creep rate only at the beginning of the inelastic process. One may verify that if $c_{\mathrm{h}} \gg 1$ then this term can be neglected. Then we obtain the kinematic hardening/recovery model proposed in Frederick and Armstrong (2007), see Sect. 3.5.2. Therefore, the variable β can be termed backstress or kinematic stress.

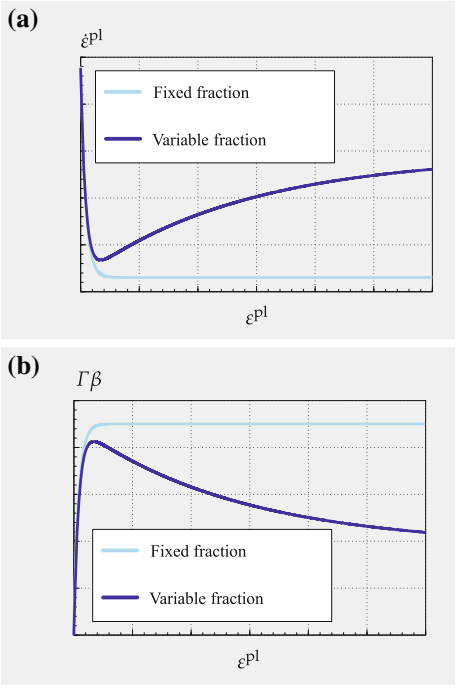

Fig. 3.6 Simulation of creep response under constant stress with Eqs. (3.5.104) and (3.5.106). **a** Qualitative variation of inelastic strain rate versus inelastic strain. **b** Qualitative variation of backstress versus inelastic strain

For the variable Γ an additional evolution equation is required. Let us assume that Γ evolves by the exponential law with the increase of the mean inelastic strain towards the saturation value $\Gamma_*(\sigma)$, i.e.

$$\dot{\Gamma} = A_{\mathrm{s}}(\Gamma_* - \Gamma)|\dot{\varepsilon}^{\mathrm{pl}}|, \tag{3.5.106}$$

where A_{s} is a constant. Then the set of Eqs. (3.5.104) and (3.5.106) describes the decrease of the inelastic strain rate as a result of stress redistribution between the constituents and the increase of the inelastic strain rate as a consequence of softening processes (decrease of the volume fraction of the hard constituent). As an example, consider a creep regime under the constant stress. Figure 3.6a illustrates the time variation of the inelastic strain rate as a function of the inelastic strain. Equations (3.5.104) and (3.5.106) describe the primary and the tertiary creep stages as a result of hardening and softening processes. If the volume fraction η_{h} is kept constant, and consequently $\Gamma = 1$, only the primary and the secondary creep stages can be described. In this case the backstress $\beta\Gamma$ attains a saturation value, Fig. 3.6b. If the volume fraction of the hard constituent is assumed to decrease, then Γ decreases and the backstress $\beta\Gamma$ decreases providing a possibility to describe the softening process. Equations (3.5.104) and (3.5.106) were identified in Naumenko et al. (2011a, b) based on creep data for several martensitic steels. Verification examples are presented illustrating a good performance of the model in describing hardening and softening for different loading paths.

3.5.4 Ageing

Strength characteristics of many materials is determined by precipitation and dispersion hardening. Heat-resistant steels contain several kinds of precipitate particles in the matrix and at grain boundaries including carbonitrides and intermetallic compounds (Abe 2008). Age-hardened aluminium alloys for high temperature applications, for example AA2014 alloy includes the θ' phase, in the form of rod-like precipitates aligned along the <001> crystallographic directions of the α-Al matrix (Naumenko and Gariboldi 2014). Dispersed fine precipitates are obstacles for mobile dislocations. Several mechanisms for interaction between mobile dislocations and particles are reviewed in Ilschner (1973), Kassner and Pérez-Prado (2004), Roesler et al. (2007) among others. An example is the Orowan bypassing mechanism, that predicts the yield stress to be inversely proportional to the mean spacing between particles or mean particle size, see Sect. 1.3. A decrease of the particle size would provide an increase of the yield stress. On the other hand, small particles can be sheared by dislocation. This shearing mechanism suggests the yield stress to decrease with a decrease in the particle size. The optimum strengthening can be achieved when an alloy contains precipitates that small enough to be bypassed and large enough to resist against shearing Roesler et al. (2007), Polmear (1996, 2004). The microstructural stability of many materials depends essentially on the precipitation sequences. For example, for age-hardenable Al alloys the high temperature exposure leads to the completion of precipitation and to coarsening of θ' particles (Gariboldi and Casaro 2007). Coarsening of carbide precipitates for steels is documented in (Abe 2008; Blum 2008; Straub 1995). The driving force of the coarsening process is the decrease in the mean surface energy. For example, for spherical particles the surface to the volume ratio is proportional to $1/D$, where D is the mean particle diameter. The increase of D would lead to a decrease of the surface energy. The process occurs by the growth of large particles at the expense of smaller ones which dissolve and is related to the diffusive mass transport. For example, the coarsening mechanism of θ' particles is governed by the diffusion of Cu in Al.

To describe the increase of the mean particle size the following equation is applied in Abe (2008), Blum (2008), Straub (1995), Gariboldi and Casaro (2007)

$$D^m = D_0^m + K(T)t, \quad K(T) = K_0 \exp\left(\frac{-Q_c}{RT}\right), \tag{3.5.107}$$

where K_0 is a material property and Q_c is the activation energy for the coarsening process. For spherical particles the exponent m takes the value 3, which is in accordance with the coarsening theories of Lifshitz and Slyozov (1961), Wagner (1961). For rod-like and plate-like particles m can take the value 2, as documented in Zhang et al. (2013), Gariboldi and Casaro (2007) for aluminum alloys. According to Eq. (3.5.107) the coarsening process is only related to the exposure time at high temperature. In several papers, for example, Nakajima et al. (2004) experimental data are presented, illustrating that inelastic deformation may affect the diffusion, and as a consequence the coarsening rate.

Though the evolution of the mean particle size can be examined by transmission electron microscopy, experimental analysis of how the mean particle size affects the inelastic strain rate is more challenging. Indeed, particles may affect the inelastic process directly and indirectly, as discussed by Ilschner (1973). The strain rate can be directly influenced by the mean particle spacing if the Orowan-type bypassing mechanism is assumed. As the particle volume fraction remains constant, the particle size is proportional to the particle spacing, see Sect. 1.3. Following Estrin (1996) the drag stress $\bar{\sigma}$ can be assumed as a superposition of the dislocation density and the particle hardening contributions as follows

$$\hat{\sigma} = MGb\left(\zeta\sqrt{\varrho} + \chi\frac{1}{D}\right), \tag{3.5.108}$$

where ζ and χ are weighting factors characterizing the contribution of the Taylor-type hardening due to dislocations and the Orowan-type hardening due to particles. With Eqs. (3.5.62) and (3.5.108) the increase in particle size leads to a decrease in the drag stress and increase in the creep rate. The particle hardening drag stress value is usually lower than the Orowan stress. This is explained by a variety of dislocation-particle interaction mechanisms operating in the creep range, e.g. dislocation climb over particles (Kassner and Pérez-Prado 2004).

Furthermore, the spacing or size of particles may affect the rates of hardening, recovery and softening. This constitutes an indirect influence on the inelastic strain rate, as pointed out by Ilschner (1973). For example, in the creep range, particles immobilize dislocations leading to formation of dislocation substructures. The storage/immobilization of dislocations can be related to the mean particle spacing.

Let us include the particle coarsening process into the constitutive equation for the inelastic strain rate and into the evolution equation for the dislocation density-type hardening variable given in Sect. 3.5.1. To this end let us modify the evolution equation for the mean dislocation density (3.5.76) as follows

$$\dot{\varrho} = \left(k_1\sqrt{\varrho} - k_2\varrho\right)|\dot{\varepsilon}^{\mathrm{pl}}|, \tag{3.5.109}$$

where

$$k_1 = 2B\sqrt{\varrho_*}, \quad k_2 = 2B, \quad \sqrt{\varrho_*} = \sqrt{\varrho_\infty}\frac{D_0}{D},$$

where D_0 is the mean particle size in the reference state. To describe the coarsening mechanism within the framework of continuum mechanics let us introduce the internal state variable $\Phi = D_0/D$ as proposed by Dyson and McLean (1998). From Eq. (3.5.107) the following kinetic equation can be derived

$$\dot{\Phi} = -\frac{A_s}{m}\Phi^{m+1}, \quad A_s(T) = A_0\exp\left(\frac{-Q_c}{RT}\right), \quad A_0 = \frac{K_0}{D_0^m} \tag{3.5.110}$$

Furthermore let us introduce a hardening variable H as follows

$$H = \frac{\zeta D\sqrt{\rho} + \chi}{\zeta D_0\sqrt{\rho_0} + \chi} \tag{3.5.111}$$

With the introduced state variables Φ and H and with Eq. (3.5.108) the constitutive equation (3.5.62) takes the following form

$$\dot{\varepsilon}^{\mathrm{pl}} = \dot{\varepsilon}_0 \left(\frac{|\sigma|}{\sigma_0 H \Phi} \right)^n \mathrm{sgn}(\sigma) \tag{3.5.112}$$

with

$$\sigma_0 = MGb \left(\zeta\sqrt{\varrho_0} + \frac{\chi}{D_0} \right)$$

The evolution equation (3.5.109) can be formulated as follows

$$\dot{H} = B\,(H_\infty - H)\,|\dot{\varepsilon}^{\mathrm{pl}}| + (H - H_{D_*})\frac{\mathrm{d}}{\mathrm{d}t}\ln\Phi, \tag{3.5.113}$$

with

$$H_\infty = \frac{\zeta D_0\sqrt{\varrho_\infty} + \chi}{\zeta D_0\sqrt{\rho_0} + \chi}, \quad H_{D_*} = \frac{\chi}{\zeta D_0\sqrt{\varrho_0} + \chi}$$

The variable H can be considered as a modified hardening variable since it includes the influence of particles in addition to the mean dislocation density. Let us note that processes associated with change in dislocation density and coarsening of precipitates have usually quite different characteristic time. Therefore, two rate terms in the right-hand side of Eq. (3.5.113) may have different orders of magnitudes since the coarsening is much slower if compared to the hardening/recovery. In Dyson and McLean (2001), Kowalewski et al. (1994), Naumenko and Gariboldi (2014), Perrin and Hayhurst (1994) instead of Eq. (3.5.113) the following simplified equation for the hardening variable is used

$$\dot{H} = B\,(H_\infty - H)\,|\dot{\varepsilon}^{\mathrm{pl}}| \tag{3.5.114}$$

Assuming the creep regime with the constant tensile stress, Eqs. (3.5.110) and (3.5.114) can be integrated providing the values of internal state variables in a closed analytical form. Then with Eq. (3.5.112) the inelastic strain rate follows

$$\dot{\varepsilon}^{\mathrm{pl}} = \dot{\varepsilon}_0 \left(\frac{\sigma}{\sigma_0} \right)^n \frac{(1 + A_s t)^{\frac{n}{m}}}{\left[H_\infty - (H_\infty - 1)\exp\left(-B\varepsilon^{\mathrm{pl}}\right) \right]^n} \tag{3.5.115}$$

Equation (3.5.115) can be used to identify the material parameters A_s, B and σ_0 as well as the functions H_∞ and $\dot{\varepsilon}_0$ from families of creep curves. An example of identification for forged AA2014 alloy is presented in Naumenko and Gariboldi (2014).

Advanced high-temperature materials, for example, high-chromium steel contain different types of precipitates having different coarsening rates. Furthermore, change in precipitation structures at grain or subgrain boundaries may promote strain softening and damage processes. For example, coarsening of precipitates at subgrain boundaries increase the rate at which subgrains coarsen. Kinetic equations for coarsening of different types of precipitates are discussed in the literature, a review presented by Straub (1995).

3.6 Damage

Softening and ageing phenomena discussed in Sects. 3.5.3 and 3.5.4 lead to a decrease of resistance against inelastic flow. As the inelastic strain rate increases and a specimen may fail as a result of necking, softening and ageing may be classified as material degradation processes. Inelastic deformation is often accompanied by damage processes—phenomena that can lead directly to macroscopic fracture. Examples include the formation, growth and coalescence of voids on grain boundaries, microcracks in particles of the second phase, decohesion at particle/matrix interfaces and surface relief. Defects in microstructure like voids and cracks may exist after the material processing, may nucleate in the early stages of loading, for example, during primary creep stage or even under spontaneous deformation in elastic range. The initially existing micro-defects have negligible influence on the macroscopic response such as inelastic strain rate. As their number and size increase, they weaken the material providing the decrease in the load-bearing capacity. The coalescence of cavities or propagation of micro-cracks lead to the final fracture. Damage mechanisms and damage processes are reviewed and classified in Ashby et al. (1979), François et al. (2012).

A micromechanics approach to damage modeling requires the analysis of many different mechanisms that may operate and interact in a specific material under specific loading conditions. As an example, consider different physical models related to grain boundary cavitation in the creep range, as discussed and reviewed in Kassner and Hayes (2003), Riedel (1987), François et al. (2012), Ozhoga-Maslovskaja et al. (2015).

A pragmatic approach is to introduce internal state variables to capture damage process in a phenomenological sense. For example, the tertiary creep stage is partly determined by the damage processes, Sect. 1.1.1.2. Therefore, one may develop and calibrate a damage evolution equation to describe the final stage of the creep curve. The idea of continuum damage mechanics is to formulate such damage laws to capture material behavior under various loading paths (Krajcinovic 1996; Lemaitre and Desmorat 2005; Murakami 2012).

3.6.1 Kachanov-Rabotnov Model

The phenomenological damage equations were firstly proposed by Kachanov (1958) and Rabotnov (1959) in order to characterize creep damage evolution. A new internal variable has been introduced to characterize "continuity" or "damage" of the material. The geometrical interpretation of the continuity variable starts from changes in the cross-section area of a uni-axial specimen. Specifying the initial cross-section area of a specimen by A_0 and the area of voids, cavities, micro-cracks, etc. by A_D, the Kachanov's continuity is defined as follows (Kachanov 1986),

$$\psi = \frac{A_0 - A_D}{A_0}$$

The value $\psi = 1$ means the virgin, fully undamaged state, the condition $\psi = 0$ corresponds to the fracture (completely damaged cross-section).

Rabotnov (1959, 1963, 1969) introduced the dual damage variable ω. In Rabotnov (1963) he pointed out that the damage state variable ω "may be associated with the area fraction of cracks, but such an interpretation is connected with a rough scheme and is therefore not necessary". Rabotnov assumed that the creep rate is additionally dependent on the current damage state. The constitutive equation should have the form

$$\dot{\varepsilon}^{\mathrm{pl}} = f(\sigma, \omega) \tag{3.6.116}$$

Furthermore, the damage processes can be reflected in the evolution equation

$$\dot{\omega} = g(\sigma, \omega), \quad \omega|_{t=0} = 0, \quad \omega < \omega_*, \tag{3.6.117}$$

where ω_* is the critical value of the damage parameter for which the material fails. With the power functions of stress and damage the constitutive equation may be formulated as follows

$$\dot{\varepsilon}^{\mathrm{pl}} = \frac{a|\sigma|^n}{(1-\omega)^m}\mathrm{sgn}\sigma \tag{3.6.118}$$

Similarly, the damage rate can be expressed by

$$\dot{\omega} = \frac{b}{(1-\omega)^l}\left(\frac{\sigma + |\sigma|}{2}\right)^k \tag{3.6.119}$$

The material dependent parameters a, b, n, m, l and k should be identified from families of creep curves. It is easy to prove that for the damage free state ($\omega = 0$), the first equation results in the power law creep constitutive equation.

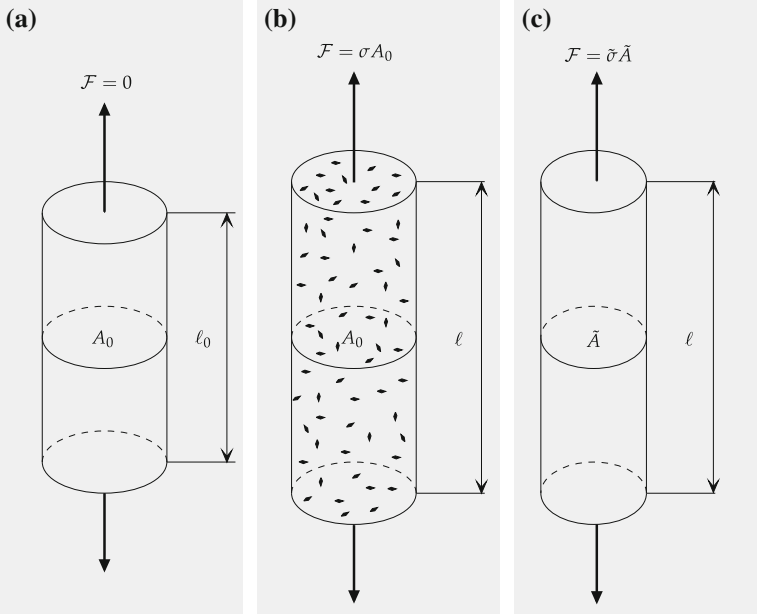

Fig. 3.7 Strain and damage of a bar. **a** Initial state. **b** Damaged state. **c** Fictitious undamaged state

Setting $m = n$ the first equation can be written as

$$\dot{\varepsilon}^{\mathrm{pl}} = a|\tilde{\sigma}|^n, \tag{3.6.120}$$

where $\tilde{\sigma} = \sigma/(1-\omega)$ is the so-called net-stress or effective stress. With the effective stress Eq. (3.6.120) provides a way to generalize a secondary creep law for the description of tertiary creep process. Lemaitre and Chaboche (1990) proposed the effective stress concept to formulate constitutive equations for damaged materials based on available constitutive equation for "virgin" materials. An interpretation can be given for a tension bar, Fig. 3.7. Here A_0 denotes the initial cross-section area of the bar, Fig. 3.7a. From the given tensile force $\mathcal{F}$ the stress can be computed as $\sigma = \mathcal{F}/A_0$. The axial strain for the loaded bar $\varepsilon = (\ell - \ell_0)/\ell_0$ can be expressed as a function of the stress and the actual damage $\varepsilon = f(\sigma, \omega)$, Fig. 3.7b. For the effective cross-section $\tilde{A} = A_0(1-\omega)$ the effective stress is

$$\tilde{\sigma} = \frac{\mathcal{F}}{\tilde{A}} = \frac{\sigma}{1-\omega} \tag{3.6.121}$$

Now a fictitious undamaged bar with a cross-section area $\tilde{A}$, Fig. 3.7c, having the same axial strain response as the actual damaged bar $\varepsilon = f(\tilde{\sigma}) = f(\sigma, \omega)$ is introduced. The strain equivalence principle (Lemaitre 1996) states that any strain constitutive equation for a damaged material may be derived in the same way as for

a virgin material except that the usual stress is replaced by the effective stress. Thus the constitutive equation for the creep rate (3.6.120) is the power law generalized for a damaged material. Note that the effective cross section area is not just understood as the initial area minus the area occupied by defects. This quantity and the effective stress are introduced to account for stress concentrations produced by cavities and/or microckracks in a phenomenological sense.

Equations (3.6.118) and (3.6.119) can be generalized to the non-isothermal conditions by replacing the parameters a and b by the functions of temperature. Assuming Arrhenius type temperature dependence the following relations can be applied

$$a(T) = a_0 \exp\left(-\frac{Q_a}{RT}\right), \quad b(T) = b_0 \exp\left(-\frac{Q_b}{RT}\right), \tag{3.6.122}$$

where Q_a and Q_b are the activation energies of creep and damage processes, respectively.

To identify the material parameters in Eqs. (3.6.118), (3.6.119) and (3.6.122) experimental data of uni-axial creep up to rupture for certain stress and temperature ranges are required. To illustrate the idea of identification let us ignore hardening, softening and ageing processes. Furthermore let us assume $m = n$ in Eq. (3.6.118) for the sake of brevity. Then the uni-axial creep model for $\sigma > 0$ takes the following form

$$\dot{\varepsilon}^{\mathrm{pl}} = a\left(\frac{\sigma}{1-\omega}\right)^n, \quad \dot{\omega} = \frac{b\sigma^k}{(1-\omega)^l} \tag{3.6.123}$$

With $\omega = 0$ the first equation describes the secondary creep. The minimum (steady-state) creep rate is defined by the power law function of the applied stress

$$\dot{\varepsilon}^{\mathrm{pl}}_{\mathrm{min}} = a\sigma^n \tag{3.6.124}$$

In the steady-state creep range the creep curves are approximated by straight lines, Fig. 3.8a. From the family of creep curves the minimum creep rate versus stress curve can be obtained. A sketch for such a curve in a double logarithmic scale is presented in Fig. 3.8b. For a certain stress range $\log \dot{\varepsilon}^{\mathrm{pl}}_{\mathrm{min}}$ can be approximated by a linear function of $\log \sigma$. The parameters a and n can be determined from the steady-state creep. Let $\dot{\varepsilon}^{\mathrm{pl}}_{\mathrm{min1}}$ and $\dot{\varepsilon}^{\mathrm{pl}}_{\mathrm{min2}}$ be minimum creep rates for the constant stresses σ_1 and σ_2, respectively. Then the material parameters can be estimated as follows

$$n = \frac{\log(\dot{\varepsilon}^{\mathrm{pl}}_{\mathrm{min1}}/\dot{\varepsilon}^{\mathrm{pl}}_{\mathrm{min2}})}{\log(\sigma_1/\sigma_2)}, \qquad a = \frac{\dot{\varepsilon}^{\mathrm{pl}}_{\mathrm{min1}}}{\sigma_1^n} = \frac{\dot{\varepsilon}^{\mathrm{pl}}_{\mathrm{min2}}}{\sigma_2^n} \tag{3.6.125}$$

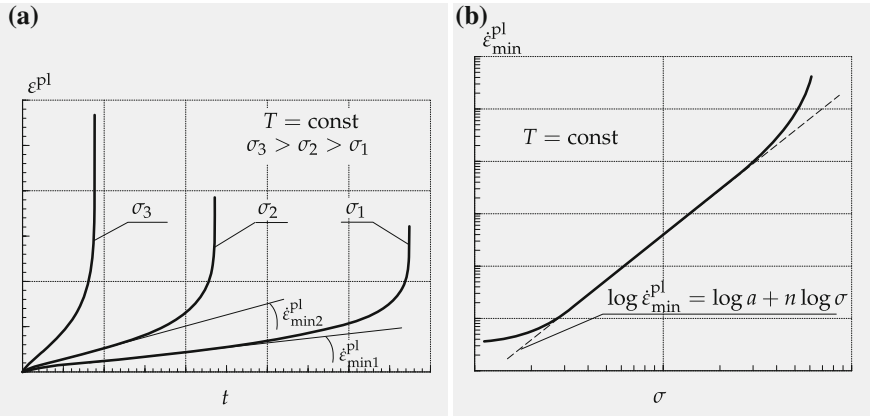

Fig. 3.8 Phenomenological description of uni-axial creep. **a** Creep strain versus time curves. **b** Minimum creep rate versus stress curve

For a constant stress σ the damage evolution equation in Eq. (3.6.123) can be integrated as follows

$$\int_0^{\omega_*} (1-\omega)^l \mathrm{d}\omega = \int_0^{t_*} b\sigma^k \mathrm{d}t,$$

where t_* is the time to fracture of the specimen. Setting $\omega_* = 1$ and performing the integration one can obtain

$$t_* = \frac{1}{(l+1)b\sigma^k} \tag{3.6.126}$$

This equation describes the time to creep fracture versus applied stress relation. For a number of metals and alloys experimental data for creep strength can be approximated by a straight line in a double logarithmic scale for a certain stress range. From Eq. (3.6.126) it follows

$$\log t_* = -(\log C + k \log \sigma), \qquad C = b(l+1) \tag{3.6.127}$$

A typical creep strength curve is sketched in Fig. 3.9. The linear approximation (3.6.127) is only valid for a specific stress range, Fig. 3.9. Based on Eq. (3.6.127) and the creep strength curve the following relations can be obtained

$$k = \frac{\log(t_{*2}/t_{*1})}{\log(\sigma_1/\sigma_2)}, \qquad b(l+1) = \frac{1}{t_{*1}\sigma_1^k} = \frac{1}{t_{*2}\sigma_2^k},$$

where t_{*1} and t_{*2} are values of time to fracture corresponding to the applied stresses σ_1 and σ_2, respectively. Integration of the second Eq. (3.6.123) by use of Eq. (3.6.126)

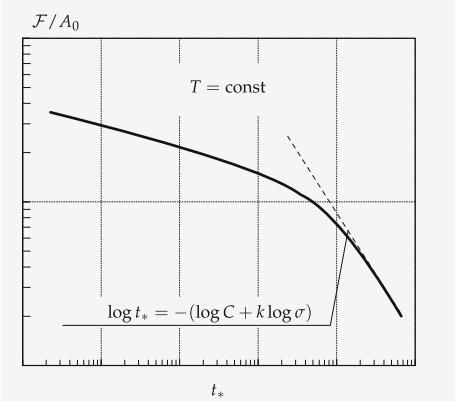

Fig. 3.9 Creep strength curve

provides the damage parameter as a function of time

$$\omega(t) = 1 - \left(1 - \frac{t}{t_*}\right)^{\frac{1}{l+1}} \tag{3.6.128}$$

With Eq. (3.6.128) the creep rate equation (3.6.123) can be integrated leading to the creep strain versus time dependence

$$\varepsilon^{\text{pl}}(t) = \frac{a\sigma^{n-k}}{b(l+1-n)}\left[1 - \left(1 - \frac{t}{t_*}\right)^{\frac{l+1-n}{l+1}}\right] \tag{3.6.129}$$

From Eq. (3.6.129) it follows that the constant l must satisfy the condition $l > n-1$ providing the positive strain for the positive stress values. By setting $t = t_*$ the creep strain before the fracture, i.e. $\varepsilon_*^{\text{pl}} = \varepsilon^{\text{pl}}(t_*)$, can be calculated as

$$\varepsilon_*^{\text{pl}} = \frac{a\sigma^{n-k}}{b(l+1-n)} \tag{3.6.130}$$

For $n > k$ the fracture strain increases with an increase in the stress value. Such a dependence is usually observed for many alloys in the case of moderate stresses. From Eqs. (3.6.124), (3.6.127) and (3.6.130) the following relations can be obtained

$$\varepsilon_*^{\text{pl}} = \frac{\dot{\varepsilon}_{\min}^{\text{pl}} t_*}{1 - \frac{n}{l+1}}, \qquad \dot{\varepsilon}_{\min}^{\text{pl}} t_* = \frac{a}{b(l+1)}\sigma^{n-k} \tag{3.6.131}$$

In the special case $n = k$ the second equation in (3.6.131) reads

$$\dot{\varepsilon}_{\min}^{\text{pl}} t_* = \frac{a}{b(l+1)} = \text{const}$$

This is the Monkman-Grant relationship which states, that for a given material the product of the minimum creep rate and the time to fracture is a material constant. We observe, that the Monkman-Grant relationship follows from the Kachanov-Rabotnov model if the slopes of the minimum creep rate versus stress and the stress versus time to fracture dependencies coincide in the double logarithmic scale. In this case the strain before the creep fracture (creep ductility) should be stress independent, as it follows from the first equation in (3.6.131).

With Eq. (3.6.131) the creep strain versus time dependence (3.6.129) takes the form

$$\varepsilon^{\mathrm{pl}}(t) = \frac{\dot{\varepsilon}^{\mathrm{pl}}_{\mathrm{min}} t_*}{1 - \frac{n}{l+1}} \left[1 - \left(1 - \frac{t}{t_*} \right)^{1 - \frac{n}{l+1}} \right] \tag{3.6.132}$$

We observe that the constant l controls the shape of the tertiary creep stage. For $n/(l+1) \ll 1$ Eq. (3.6.132) can be approximated by

$$\varepsilon^{\mathrm{pl}}(t) = \dot{\varepsilon}^{\mathrm{pl}}_{\mathrm{min}} t, \quad 0 \le t \le t_*$$

In this case the tertiary creep stage is not observable. Instead of Eq. (3.6.123) one may apply the simplified constitutive model, where the influence of creep damage on the creep rate is ignored, i.e.

$$\dot{\varepsilon}^{\mathrm{pl}} = a\sigma^n, \quad \dot{\omega} = \frac{b\sigma^k}{(1-\omega)^l} \tag{3.6.133}$$

In a slightly different form Eq. (3.6.133) were originally proposed by Kachanov (1958) under assumption that for brittle materials the damage processes have negligible influence on the creep rate.

Figure 3.10 provides the plots of Eq. (3.6.132) with respect to the normalized creep strain and normalized time for different values of $r \equiv n/(l+1)$. We observe that even for $r = 0.2$ the creep rate is almost constant. The increase of r leads to the increase of tertiary creep rate, the increase of the "duration" of the tertiary stage and increase of the fracture strain.

The phenomenological model (3.6.123) characterizes the effect of damage evolution and describes the tertiary creep in a uni-axial test. For a number of metals and alloys material parameters are available, see e.g. Altenbach et al. (1997), Altenbach and Naumenko (1997), Altenbach et al. (2000, 2001), Bodnar and Chrzanowski (1991), Boyle and Spence (1983), Hayhurst (1972), Hyde et al. (2003, 2000, 1997, 1999), Konkin and Morachkovskij (1987), Kowalewski (1996), Lemaitre (2001), Lemaitre and Chaboche (1990), Lemaitre et al. (2009), Murakami and Liu (1995). Instead of the power law functions of stress or damage it is possible to use another kind of functions, e.g. the hyperbolic sine functions in both the creep and damage evolution equations. In addition, by the introduction of suitable hardening, softening and ageing variables, the model can be extended to consider all creep stages. Examples are presented in Altenbach et al. (2013), Kowalewski et al. (1994), Naumenko

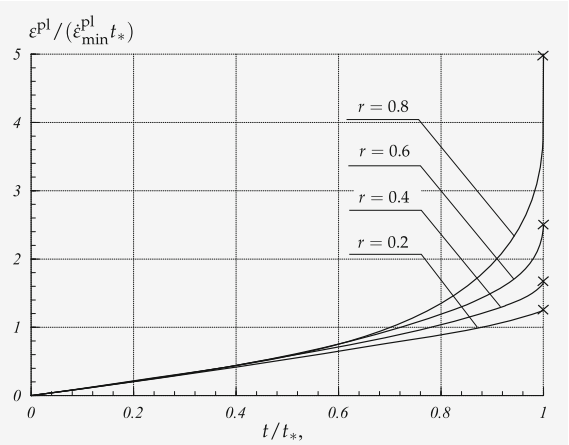

Fig. 3.10 Creep curves for different values of $r = n/(l+1)$

and Kostenko (2009), Naumenko et al. (2011a, b), Naumenko and Altenbach (2005), Perrin and Hayhurst (1994).

In applying Eq. (3.6.123) to the analysis of structures one should bear in mind that the material parameters are usually estimated from experimental creep curves, available for a narrow range of stresses. The linear dependencies between $\log \dot{\varepsilon}^{\rm cr}_{\rm min}$ and $\log \sigma$ or between $\log t_*$ and $\log \sigma$ do not hold for wide stress ranges. For example, it is known from materials science that for higher stresses the damage mode may change from inter-granular to trans-granular, e.g. Ashby et al. (1979). Furthermore, for higher values of the engineering stress the true stress increases due to the cross section shrinkage. This should be considered in calibrating the damage evolution equation based on experimental data on creep and/or creep strength. One may assume that the volume of the specimen does not change during the creep process providing the relation between the change in the cross section and the elongation, Sect. 3.4. With the relation between the true stress and the engineering stress the damage evolution equation (3.6.123) can be integrated providing a two-stage creep strength curve, Fig. 3.10. The related analysis is presented in Rabotnov (1963, 1969).

The damage evolution equation may be put in a different form, which is sometimes more convenient for the identification. To this end let us specify Eqs. (3.6.116) and (3.6.117) as follows

$$\dot{\varepsilon}^{\rm pl} = f_\sigma(|\sigma|) f_\omega(\omega) {\rm sgn}\sigma, \quad \dot{\omega} = g_\sigma(|\sigma|) g_\omega(\omega) \frac{1 + {\rm sgn}\sigma}{2}, \tag{3.6.134}$$

where $f_\sigma(|\sigma|)$, $f_\omega(\omega)$, $g_\sigma(|\sigma|)$ and $g_\omega(\omega)$ are functions to be identified from experimental data. With the constitutive equation for the inelastic strain rate $(3.6.134)_1$ the damage evolution equation $(3.6.134)_2$ can be put in the following form

$$\dot{\omega} = h_\omega(\omega)\frac{1+\operatorname{sgn}\sigma}{2}\frac{|\dot{\varepsilon}^{\mathrm{pl}}|}{\varepsilon_*^{\mathrm{pl}}(|\sigma|)}, \tag{3.6.135}$$

where

$$h_\omega(\omega) = \frac{g_\omega(\omega)}{f_\omega(\omega)} r(\omega_*), \quad r(\omega_*) = \int_0^{\omega_*} \frac{f_\omega(x)}{g_\omega(x)}\mathrm{d}x, \quad \varepsilon_*(|\sigma|) = \frac{f_\sigma(|\sigma|)}{g_\sigma(|\sigma|)}$$

Integrating (3.6.135) for the constant positive true stress provides the relationship between the damage parameter and the inelastic strain

$$\Psi(\omega) = \frac{\varepsilon^{\mathrm{pl}}}{\varepsilon_*^{\mathrm{pl}}(|\sigma|)}, \tag{3.6.136}$$

where

$$\Psi(\omega) = \int_0^{\omega} \frac{\mathrm{d}x}{h_\omega(x)}$$

Since $\Psi(\omega_*) = 1$, the function $\varepsilon_*^{\mathrm{pl}}(|\sigma|)$ is the strain before the creep fracture under the constant true stress.

3.6.2 Continuum Damage Mechanics

Let us discuss how to introduce a damage parameter into the one-dimensional continuum mechanics framework. For the sake of brevity let us ignore hardening, softening and ageing. The dissipation inequality (2.6.50) with $\dot{F}F^{-1} = \dot{\varepsilon}_{\mathrm{H}}$ has the following form (3.5.66)

$$\sigma\dot{\varepsilon}_{\mathrm{H}} - \rho\dot{\Phi} - \rho\mathcal{S}\dot{T} - q\frac{T'}{T} \geq 0 \tag{3.6.137}$$

Let us assume the following split of the mechanical power

$$\begin{aligned} \mathcal{L} &= \sigma\dot{\varepsilon}_{\mathrm{H}} = \mathcal{L}_{\mathrm{s}} + \mathcal{L}_{\mathrm{d}}, \\ \mathcal{L}_{\mathrm{s}} &= \sigma_{\mathrm{s}}(\varepsilon_{\mathrm{H}}^{\mathrm{el}}, \omega, T)\dot{\varepsilon}_{\mathrm{H}}^{\mathrm{el}}, \\ \mathcal{L}_{\mathrm{d}} &= \sigma_{\mathrm{d}}(\dot{\varepsilon}_{\mathrm{H}}^{\mathrm{pl}}, \omega, T)\dot{\varepsilon}_{\mathrm{H}}^{\mathrm{pl}} \end{aligned} \tag{3.6.138}$$

As in the Sect. 3.5 let us assume the iso-stress approach such that

$$\sigma = \sigma_{\mathrm{s}}(\varepsilon_{\mathrm{H}}^{\mathrm{el}}, \omega, T) = \sigma_{\mathrm{d}}(\dot{\varepsilon}_{\mathrm{H}}^{\mathrm{pl}}, \omega, T)$$

Therefore, the free energy is now a function of the elastic strain, the damage parameter and the temperature. The inequality (3.5.66) takes the form

$$\left(\sigma - \rho\frac{\partial \Phi}{\partial \varepsilon_{\mathrm{H}}^{\mathrm{el}}}\right)\dot{\varepsilon}_{\mathrm{H}}^{\mathrm{el}} - \rho\left(\frac{\partial \Phi}{\partial T} + \mathcal{S}\right)\dot{T} + \sigma\dot{\varepsilon}^{\mathrm{pl}} - \rho\frac{\partial \Phi}{\partial \omega}\dot{\omega} - q\frac{T'}{T} \geq 0 \tag{3.6.139}$$

To resolve the inequality assume that the internal state variable ω is defined by the following evolution equation

$$\dot{\omega} = g(\varepsilon_{\mathrm{H}}^{\mathrm{el}}, T, \omega, \dot{\varepsilon}_{\mathrm{H}}^{\mathrm{pl}}) \tag{3.6.140}$$

Furthermore, assume that the thermal conductivity is not affected by damage, for the sake of brevity.[6] Then, for arbitrary $\dot{\varepsilon}^{\mathrm{el}}$ and $\dot{T}$ the inequality (3.6.139) is satisfied with

$$\sigma = \rho\frac{\partial \Phi}{\partial \varepsilon_{\mathrm{H}}^{\mathrm{el}}}, \quad \mathcal{S} = -\frac{\partial \Phi}{\partial T}, \quad -q\frac{T'}{T} \geq 0, \quad \sigma\dot{\varepsilon}_{\mathrm{H}}^{\mathrm{pl}} - \rho\frac{\partial \Phi}{\partial \omega}\dot{\omega} \geq 0 \tag{3.6.141}$$

For the stress let us assume the following constitutive equation

$$J\sigma = \frac{\partial \rho_0 \Phi}{\partial \varepsilon_{\mathrm{H}}^{\mathrm{el}}} = \begin{cases} E g_{\omega_{\mathrm{T}}}(\omega)\varepsilon_{\mathrm{H}}^{\mathrm{el}}, & \varepsilon_{\mathrm{H}}^{\mathrm{el}} \geq 0, \\ E g_{\omega_{\mathrm{C}}}(\omega)\varepsilon_{\mathrm{H}}^{\mathrm{el}}, & \varepsilon_{\mathrm{H}}^{\mathrm{el}} < 0, \end{cases} \tag{3.6.142}$$

where the functions $g_{\omega_{\mathrm{T}}}(\omega)$ and $g_{\omega_{\mathrm{C}}}(\omega)$ have the following properties

$$g_{\omega_i}(0) = 1, \quad g_{\omega_i}(\omega_*) = g_{*_i}, \quad 0 < g_{*_i} \ll 1, \quad \frac{dg_{\omega_i}}{d\omega} \leq 0, \quad i = \mathrm{T}, \mathrm{C}$$

These functions characterize the degradation of stiffness with progressive damage. As different damage mechanisms under tension and compression operate, different functions with subscripts T and C for tensile and compressive regimes are introduced. The material parameters $g_{*_{\mathrm{T}}}$ and $g_{*_{\mathrm{C}}}$ are introduced to evaluate the material stiffness under the critical damage state. Equation (3.6.142) can also be formulated as follows

$$J\sigma = E g_{\omega_{\mathrm{T}}}(\omega)\frac{\varepsilon_{\mathrm{H}}^{\mathrm{el}} + |\varepsilon_{\mathrm{H}}^{\mathrm{el}}|}{2} + E g_{\omega_{\mathrm{C}}}(\omega)\frac{\varepsilon_{\mathrm{H}}^{\mathrm{el}} - |\varepsilon_{\mathrm{H}}^{\mathrm{el}}|}{2} \tag{3.6.143}$$

With the constitutive equation (3.6.142), Eq. (3.6.141) can be integrated providing the following expression for the free energy

[6] The influence of damage on the heat transfer is analyzed in Skrzypek and Ganczarski (1998), Ganczarski and Skrzypek (2000).

$$\rho_0\Phi = \left\{ \begin{array}{l} \frac{1}{2} E g_{\omega_\mathrm{T}}(\omega)\varepsilon_\mathrm{H}^{\mathrm{el}^2}, \ \varepsilon_\mathrm{H}^\mathrm{el} \geq 0 \\ \frac{1}{2} E g_{\omega_\mathrm{C}}(\omega)\varepsilon_\mathrm{H}^{\mathrm{el}^2}, \ \varepsilon_\mathrm{H}^\mathrm{el} < 0 \end{array} \right\} + \rho_0\Phi_\omega(\omega) + \rho_0\Phi_0, \tag{3.6.144}$$

where $\rho_0\Phi_\omega(\omega)$ is the energy required to damage an infinitesimal volume element up to the value ω. It can be interpreted, as the energy required to form cavities of given radius and distribution, energy to form microcracks of given length and distribution, etc. With (3.6.144) the last inequality in (3.6.141) takes the following form

$$J\sigma\dot{\varepsilon}_\mathrm{H}^\mathrm{pl} + R(\varepsilon_\mathrm{H}^\mathrm{el}, \omega)\dot{\omega} \geq 0, \quad R(\varepsilon_\mathrm{H}^\mathrm{el}, \omega) = Y(\varepsilon_\mathrm{H}^\mathrm{el}, \omega) - h(\omega), \tag{3.6.145}$$

where

$$Y = -\frac{1}{2} E \varepsilon_\mathrm{H}^{\mathrm{el}^2} \left\{ \begin{array}{l} \frac{\mathrm{d}g_{\omega_\mathrm{T}}}{\mathrm{d}\omega}, \ \varepsilon_\mathrm{H}^\mathrm{el} \geq 0, \\ \frac{\mathrm{d}g_{\omega_\mathrm{C}}}{\mathrm{d}\omega}, \ \varepsilon_\mathrm{H}^\mathrm{el} < 0, \end{array} \right. \qquad h(\omega) = \frac{\mathrm{d}\rho_0\Phi_\omega}{\mathrm{d}\omega}, \tag{3.6.146}$$

The degradation functions g_{ω_T}, g_{ω_C}, the resistance function $h(\omega)$ as well as the damage evolution equation should be specified according to mechanisms of damage evolution for the given material, loading conditions and results of material testing. Many formulations related to brittle damage, ductule damage, creep damage, fatigue damage are discussed within the framework of continuum damage mechanics (Murakami 2012; Lemaitre and Desmorat 2005; Skrzypek and Ganczarski 1998). Let us consider some elementary examples.

With the strain equivalence principle, Sect. 3.6.1 the degradation functions can be given as follows, e.g. Lemaitre and Desmorat (2005)

$$g_{\omega_\mathrm{T}} = 1 - \omega, \quad g_{\omega_\mathrm{C}} = 1 - \kappa\omega, \quad 0 \leq \omega \leq \omega_*, \quad 0 \leq \kappa \leq 1 \tag{3.6.147}$$

where $\omega_* < 1$ is a critical value of the damage parameter, and the constant κ controls the tension-compression difference caused by damage. For $\kappa = 0$, damage does not affect the strain energy density under compression while for $\kappa = 1$ the behavior under tension and compression is the same. Let us assume $h(\omega) = h_0$, where h_0 is a constant. Furthermore, let us neglect the inelastic behavior and consider small elastic strains. Then the inequality (3.6.145) takes the following form

$$R(\varepsilon)\dot{\omega} \geq 0, \quad R(\varepsilon) = \left\{ \begin{array}{l} \frac{1}{2} E\varepsilon^2 - h_0, \quad \varepsilon \geq 0, \\ \frac{1}{2}\kappa E\varepsilon^2 - h_0, \ \varepsilon < 0 \end{array} \right. \tag{3.6.148}$$

Assume that $\dot{\omega} \geq 0$, i.e. damage healing processes are excluded. Then the dissipation inequality (3.6.148) can be satisfied with the following damage evolution equation

$$\dot{\omega} = \Omega(< R(\varepsilon) >), \tag{3.6.149}$$

where $\Omega(x)$ is a monotonic function with $\Omega(x) \geq 0$ and $\Omega(0) = 0$. The Macaulay brackets $<>$ are defined as follows

$$< x >= \frac{x + |x|}{2}$$

The function $R(\varepsilon)$ plays a role of a damage driving force similarly to the concept of crack driving force in the fracture mechanics (Rice 1978). An example for Ω is a power law-type function

$$\dot{\omega} = a_0 \left(\frac{< R(\varepsilon) >}{R_0} \right)^p, \tag{3.6.150}$$

where a_0, R_0 and p are material parameters. Instead of (3.6.150) one may apply a rate-independent formulation which includes the condition of the non-negative damage rate, i.e. $\dot{\omega} \geq 0$ and the admissibility condition for the diving force, i.e. $R(\varepsilon) \leq 0$. Furthermore it is assumed that $\dot{\omega} = 0$ if $R(\varepsilon) < 0$ and $\dot{\omega} > 0$ is only possible if $R(\varepsilon) = 0$. The rate-independent formulation can be given as follows

$$\dot{\omega} \geq 0, \quad R(\varepsilon) \leq 0, \quad \dot{\omega} R(\varepsilon) = 0 \tag{3.6.151}$$

With Eq. (3.6.143) one can compute the stress as follows

$$\sigma = E(1 - \omega) \frac{\varepsilon + |\varepsilon|}{2} + E(1 - \kappa\omega) \frac{\varepsilon - |\varepsilon|}{2} \tag{3.6.152}$$

Equations (3.6.148)–(3.6.152) can be used to model elasticity with damage based on the strain energy density criterion for damage evolution. Instead of the strain energy density one may apply the complementary energy density. The inverse of Eg. (3.6.152) provides

$$\varepsilon = \frac{\sigma + |\sigma|}{2E(1 - \omega)} + \frac{\sigma - |\sigma|}{2E(1 - \kappa\omega)} \tag{3.6.153}$$

Inserting into Eq. (3.6.148) yields the following stress based formulation

$$R_\sigma(\sigma, \omega)\dot{\omega} \geq 0, \quad R_\sigma(\sigma, \omega) = \begin{cases} \dfrac{\sigma^2}{2E(1 - \omega)^2} - h_0, & \sigma \geq 0, \\ \dfrac{\kappa\sigma^2}{2E(1 - \kappa\omega)^2} - h_0, & \sigma < 0 \end{cases} \tag{3.6.154}$$

The damage driving force $R_\sigma(\sigma, \omega)$ can also be given as follows

$$R_\sigma(\sigma, \omega) = \frac{\sigma^2}{2E(1 - \omega)^2} \left[\frac{1 + \text{sgn}\sigma}{2} + \kappa \frac{1 - \text{sgn}\sigma}{2} \left(\frac{1 - \omega}{1 - \kappa\omega} \right)^2 \right] - h_0 \tag{3.6.155}$$

With Eq. (3.6.155) the damage evolution equation can be formulated with respect to the stress. Depending on the type of material behavior and available experimental data different forms of damage evolution equations for brittle materials are proposed. The difference is in the type of the degradation functions, the type of damage resistance functions and the type of the damage driving force (Murakami 2012; Lemaitre and Desmorat 2005; Skrzypek and Ganczarski 1998).

To present examples of damage evolution equations for materials that exhibit inelastic material behavior let us apply the stress-based formulation. To this end we apply the inverse form of the constitutive equation (3.6.143)

$$\varepsilon_{\mathrm{H}}^{\mathrm{el}}(\sigma,\omega) = J\frac{\sigma+|\sigma|}{2Eg_{\omega_{\mathrm{T}}}(\omega)} + J\frac{\sigma-|\sigma|}{2Eg_{\omega_{\mathrm{C}}}(\omega)} \tag{3.6.156}$$

For the sake of brevity let us assume that under compression the effect of damage is negligible and set $g_{\omega_{\mathrm{C}}}(\omega) = 1$. With Eq. (3.6.156) the dissipation inequality (3.6.145) can be formulated as follows

$$J\sigma\dot{\varepsilon}_{\mathrm{H}}^{\mathrm{pl}} + R_\sigma(\sigma,\omega)\dot{\omega} \geq 0, \quad R_\sigma(\sigma,\omega) = Y_\sigma(\sigma,\omega) - h(\omega), \tag{3.6.157}$$

where

$$Y_\sigma(\sigma,\omega) = -\frac{1}{2E}\left(\frac{J\sigma}{g_{\omega_{\mathrm{T}}}}\right)^2 \frac{\mathrm{d}g_{\omega_{\mathrm{T}}}}{\mathrm{d}\omega}\left(\frac{1+\mathrm{sgn}\sigma}{2}\right) \tag{3.6.158}$$

Many constitutive models of inelastic behavior coupled with damage that satisfy (3.6.157) were proposed, e.g. Murakami (2012), Lemaitre and Desmorat (2005), Skrzypek and Ganczarski (1998). One example is the following formulation

$$\dot{\varepsilon}^{\mathrm{pl}} = f_\sigma(|\sigma|)f_\omega(\omega)\mathrm{sgn}\sigma, \quad \dot{\omega} = \Omega(< R_\sigma >)|\dot{\varepsilon}^{\mathrm{pl}}| \tag{3.6.159}$$

To specify the response functions f_σ, f_ω, Ω, $g_{\omega_{\mathrm{T}}}$ and h experimental data are required. As an example consider the following functions

$$\begin{aligned} f_\sigma(x) &= a\left(\frac{x}{\sigma_0}\right)^n, \quad f_\omega(x) = (1-x)^{-m}, \\ \Omega(x) &= b\left(\frac{x}{R_0}\right)^k, \quad g_{\omega_{\mathrm{T}}}(x) = (1-x), \quad h(x) = h_0, \end{aligned}$$

where a, b, σ_0, R_0, h_0, n and k are material parameters. Equations (3.6.159) take the following form

$$\begin{aligned} \dot{\varepsilon}^{\mathrm{pl}} &= a\left(\frac{|\sigma|}{\sigma_0}\right)^n \frac{1}{(1-\omega)^m}\mathrm{sgn}\sigma, \\ \dot{\omega} &= b\left(\frac{< R_\sigma >}{R_0}\right)^k |\dot{\varepsilon}^{\mathrm{pl}}|, \quad R_\sigma = \frac{1}{2E}\left(\frac{J\sigma}{1-\omega}\right)^2 - h_0 \end{aligned} \tag{3.6.160}$$

References

Abe F (2008) Strengthening mechanisms in steel for creep and creep rupture. In: Abe F, Kern TU, Viswanathan R (eds) Creep-resistant steels. Woodhead Publishing, Cambridge, pp 279–304

Abe F (2009) Analysis of creep rates of tempered martensitic 9% Cr steel based on microstructure evolution. Mater Sci Engi: A 510:64–69

Altenbach H, Naumenko K (1997) Creep bending of thin-walled shells and plates by consideration of finite deflections. Comput Mech 19:490–495

Altenbach H, Morachkovsky O, Naumenko K, Sychov A (1997) Geometrically nonlinear bending of thin-walled shells and plates under creep-damage conditions. Arch Appl Mech 67:339–352

Altenbach H, Altenbach J, Naumenko K (1998) Ebene Flächentragwerke. Springer, Berlin

Altenbach H, Kolarow G, Morachkovsky O, Naumenko K (2000) On the accuracy of creep-damage predictions in thinwalled structures using the finite element method. Comput Mech 25:87–98

Altenbach H, Kushnevsky V, Naumenko K (2001) On the use of solid- and shell-type finite elements in creep-damage predictions of thinwalled structures. Arch Appl Mech 71:164–181

Altenbach H, Gorash Y, Naumenko K (2008a) Steady-state creep of a pressurized thick cylinder in both the linear and the power law ranges. Acta Mech 195:263–274

Altenbach H, Naumenko K, Gorash Y (2008b) Creep analysis for a wide stress range based on stress relaxation experiments. Int J Mod Phys B 22:5413–5418

Altenbach H, Kozhar S, Naumenko K (2013) Modeling creep damage of an aluminum-silicon eutectic alloy. Int J Damage Mech 22(5):683–698

Antman SS (1973) Nonuniqueness of equilibrium states for bars in tension. J Math Anal Appl 44(2):333–349

Ashby MF, Gandhi C, Taplin DMR (1979) Fracture-mechanism maps and their construction for f.c.c. metals and alloys. Acta Metall 27:699–729

Barkar T, Ågren J (2005) Creep simulation of 9–12%Cr steels using the composite model with thermodynamically calculated input. Mater Sci Eng A 395:110–115

Bertram A (2012) Elasticity and plasticity of large deformations, 3rd edn. Springer, Berlin

Besseling JF (1958) A theory of elastic, plastic and creep deformation of an initially isotropic material showing anisotropic strain hardening, creep recovery and secondary creep. Trans ASME J Appl Mech 25(1):529–536

Besseling JF, van der Giessen E (1994) Mathematical modelling of inelastic deformation. Chapman & Hall, London

Blum W (2008) Mechanisms of creep deformation in steel. In: Abe F, Kern TU, Viswanathan R (eds) Creep-resistant steels. Woodhead Publishing, Cambridge, pp 365–402

Bodnar A, Chrzanowski M (1991) A non-unilateral damage in creeping plates. In: Zyczkowski M (ed) Creep in structures. Springer, Berlin, Heidelberg, pp 287–293

Boyle JT (2012) The creep behavior of simple structures with a stress range-dependent constitutive model. Arch Appl Mech 82(4):495–514

Boyle JT, Spence J (1983) Stress analysis for creep. Butterworth, London

Chaboche JL (1989) Constitutive equations for cyclic plasticity and cyclic viscoplasticity. Int J Plast 5:247–302

Chaboche JL (2008) A review of some plasticity and viscoplasticity constitutive equations. Int J Plast 24:1642–1693

Coleman BD (1986) Necking and drawing in polymeric fibers under tension. The breadth and depth of continuum mechanics. Springer, Berlin Heidelberg, pp 19–41

Coleman BD, Gurtin ME (1967) Thermodynamics with internal state variables. J Chem Phys 47(2):597–613

Courant R, Hilbert D (1989) Methods of mathematical physics, vol 2: partial differential equations. Wiley Interscience Publication, New York

Dünnwald J, El-Magd E (1996) Description of the creep behaviour of the precipitation-hardened material al-cu-mg alloy 2024 using finite element computations based on microstructure mechanical models. Comput Mater Sci 7(1):200–207

Dyson BF, McLean M (1998) Microstructural evolution and its effects on the creep performance of high temperature alloys. In: Strang A, Cawley J, Greenwood GW (eds) Microstructural stability of creep resistant alloys for high temperature plant applications. Cambridge University Press, Cambridge, pp 371–393

Dyson BF, McLean M (2001) Micromechanism-quantification for creep constitutive equations. In: Murakami S, Ohno N (eds) IUTAM symposium on creep in structures. Kluwer, Dordrecht, pp 3–16

El-Magd E, Kranz A (2000) Ermittlung der inneren Rückspannung der Aluminiumlegierung AA2024 bei Kriechbelastung. Materialwissenschaft und Werkstofftechnik 31(1):96–101

Estrin Y (1996) Dislocation-density-related constitutive modelling. In: Krausz AS, Krausz K (eds) Unified constitutive laws of plastic deformation. Academic Press, San Diego, pp 69–104

François D, Pineau A, Zaoui A (2012) Mechanical behaviour of materials, mechanical behaviour of materials, vol II: fracture mechanics and damage. Springer

Frederick CO, Armstrong PJ (2007) A mathematical representation of the multiaxial Bauschinger effect. Mater High Temp 24(1):1–26

Frost HJ, Ashby MF (1982) Deformation-mechanism maps. Pergamon, Oxford

Ganczarski A, Skrzypek J (2000) Damage effect on thermo-mechanical fields in a mid-thick plate. J Theor Appl Mech 38(2):271–284

Gariboldi E, Casaro F (2007) Intermediate temperature creep behaviour of a forged Al-Cu-Mg-Si-Mn alloy. Mater Sci Eng: A 462(1):384–388

Giesekus H (1994) Phänomenologische Rheologie. Springer, Berlin

Gould PL (1988) Analysis of shells and plates. Springer, New York

Granger R (1994) Experiments in heat transfer and thermodynamics. Cambridge University Press, Cambridge

Hahn HG (1985) Elastizitätstheorie. Teubner, Stuttgart, B.G

Hayhurst DR (1972) Creep rupture under multiaxial states of stress. J Mech Phys Solids 20:381–390

Hoff NJ (1953) The necking and the rupture of rods subjected to constant tensile loads. Trans ASME J Appl Mech 20(1):105–108

Hosseini E, Holdsworth SR, Mazza E (2013) Stress regime-dependent creep constitutive model considerations in finite element continuum damage mechanics. Int J Damage Mech. 22(8): 1186–1205

Hyde TH, Sun W, Becker AA, Williams JA (1997) Creep continuum damage constitutive equations for the base, weld and heat-affected zone materials of a service-aged 1/2Cr1/2Mo1/4V:2 1/4Cr1Mo multipass weld at 640°C. J Strain Anal Eng Des 32(4):273–285

Hyde TH, Sun W, Williams JA (1999) Creep behaviour of parent, weld and HAZ materials of new, service aged and repaired 1/2Cr1/2Mo1/4V: 21/4Cr1Mo pipe welds at 640°C. Mater High Temp 16(3):117–129

Hyde TH, Sun W, Becker AA (2000) Failure prediction for multi-material creep test specimens using steady-state creep rupture stress. Int J Mech Sci 42:401–423

Hyde TH, Sun W, Agyakwa PA, Shipeay PH, Williams JA (2003) Anisotropic creep and fracture behaviour of a 9CrMoNbV weld metal at 650°C. In: Skrzypek JJ, Ganczarski AW (eds) Anisotropic behaviour of damaged materials. Springer, Berlin, pp 295–316

Ilschner B (1973) Hochtemperatur-Plastizität. Springer, Berlin

Kachanov LM (1958) O vremeni razrusheniya v usloviyakh polzuchesti (on the time to rupture under creep conditions, in russ.). Izv AN SSSR Otd Tekh Nauk 8:26–31

Kachanov LM (1986) Introduction to continuum damage mechanics. Martinus Nijhoff, Dordrecht

Kassner ME, Hayes TA (2003) Creep cavitation in metals. Int J Plast 19:1715–1748

Kassner ME, Pérez-Prado MT (2004) Fundamentals of creep in melals and alloys. Elsevier, Amsterdam

Khan AS, Huang S (1995) Continuum theory of plasticity. Wiley, New York

Konkin VN, Morachkovskij OK (1987) Polzuchest' i dlitel'naya prochnost' legkikh splavov, proyavlyayushchikh anizotropnye svoistva (Creep and long-term strength of light alloys with anisotropic properties, in Russ.). Problemy prochnosti 5:38–42

Kowalewski ZL (1996) Creep rupture of copper under complex stress state at elevated temperature. Design and life assessment at high temperature. Mechanical Engineering Publ, London, pp 113–122
Kowalewski ZL, Hayhurst DR, Dyson BF (1994) Mechanisms-based creep constitutive equations for an aluminium alloy. J Strain Anal Eng Des 29(4):309–316
Krajcinovic D (1996) Damage mechanics. Appl Math Mech 41. North-Holland, Amsterdam
Krawietz A (1986) Materialtheorie: Mathematische Beschreibung des phänomenologischen thermomechanischen Verhalten. Springer, Berlin
Krempl E (1996) A small-strain viscoplasticity theory based on overstress. In: Krausz AS, Krausz K (eds) Unified constitutive laws of plastic deformation. Academic Press, San Diego, pp 281–318
Krempl E (1999) Creep-plasticity interaction. In: Altenbach H, Skrzypek J (eds) Creep and damage in materials and structures. Springer, Wien, New York, pp 285–348, CISM Lecture Notes No. 399
Landau LD, Lifshits EM, Kosevich AM, Pitaevskii LP (1986) Theory of elasticity. Butterworth-Heinemann, Course of theoretical physics
Längler F, Naumenko K, Altenbach H, Ievdokymov M (2014) A constitutive model for inelastic behavior of casting materials under thermo-mechanical loading. J Strain Anal Eng Des 49: 421–428
Lemaitre J (1996) A course on damage mechanics. Springer, Berlin
Lemaitre J (ed) (2001) Handbook of materials behavior models. Academic Press, San Diego
Lemaitre J, Chaboche JL (1990) Mechanics of solid materials. Cambridge University Press, Cambridge
Lemaitre J, Desmorat R (2005) Engineering damage mechanics: ductile, creep. Springer, Fatigue and Brittle Failures
Lemaitre J, Chaboche J, Benallal A, Desmorat R (2009) Mécanique deés Matériaux Solides, 3rd edn. Mechanics and thermodynamics, Dunod, Paris, The Addison-Wesley Series in the engineering sciences
Lifshitz IM, Slyozov VV (1961) The kinetics of precipitation from supersaturated solid solutions. J Phys Chem Solids 19:35–50
Lurie A (2010) Theory of elasticity. Springer, Foundations of Engineering Mechanics
Malinin NN, Khadjinsky GM (1972) Theory of creep with anisotropic hardening. Int J Mech Sci 14:235–246
Maugin GA (1992) The thermomechanics of plasticity and fracture. Cambridge University Press, Cambridge
Maugin GA (2015) The saga of internal variables of state in continuum thermo-mechanics (1893–2013). Mech Res Commun 69:79–86
Müller I (2007) A history of thermodynamics: the doctrine of energy and entropy. Springer
Murakami S (2012) Continuum damage mechanics: a continuum mechanics approach to the analysis of damage and fracture. Springer, Solid Mechanics and Its Applications
Murakami S, Liu Y (1995) Mesh-dependence in local approach to creep fracture. Int J Damage Mech 4:230–250
Nabarro FRN, de Villiers HL (1995) The physics of creep: creep and creep-resistant alloys. Taylor & Francis, London
Naghdi PM (1990) A critical review of the state of finite plasticity. J Appl Math Phys (ZAMP) 41:316–394
Nakajima T, Takeda M, Endo T (2004) Accelerated coarsening of precipitates in crept Al-Cu alloys. Mater Sci Eng: A 387:670–673
Naumenko K, Altenbach H (2005) A phenomenological model for anisotropic creep in a multi-pass weld metal. Arch Appl Mech 74:808–819
Naumenko K, Gariboldi E (2014) A phase mixture model for anisotropic creep of forged Al-Cu-Mg-Si alloy. Mater Sci Eng: A 618:368–376
Naumenko K, Kostenko Y (2009) Structural analysis of a power plant component using a stress-range-dependent creep-damage constitutive model. Mater Sci Eng A510–A511:169–174

Naumenko K, Altenbach H, Gorash Y (2009) Creep analysis with a stress range dependent constitutive model. Arch Appl Mech 79:619–630

Naumenko K, Altenbach H, Kutschke A (2011a) A combined model for hardening, softening and damage processes in advanced heat resistant steels at elevated temperature. Int J Damage Mech 20:578–597

Naumenko K, Kutschke A, Kostenko Y, Rudolf T (2011b) Multi-axial thermo-mechanical analysis of power plant components from 9–12%Cr steels at high temperature. Eng Fract Mech 78: 1657–1668

Nellis G, Klein S (2009) Heat transfer. Cambridge University Press, Cambridge

Ohno N (1998) Constitutive modeling of cyclic plasticity with emphasis on ratchetting. Int J Mech Sci 40(2):251–261

Ohno N, Abdel-Karim M, Kobayashi M, Igari T (1998) Ratchetting characteristics of 316FR steel at high temperature, Part I: strain-controlled ratchetting experiments and simulations. Int J Plast 14(4):355–372

Ozhoga-Maslovskaja O, Naumenko K, Altenbach H, Prygorniev O (2015) Micromechanical simulation of grain boundary cavitation in copper considering non-proportional loading. Comput Mater Sci 96, Part A:178–184

Palmov V (1998) Vibrations in elasto-plastic bodies. Springer, Berlin

Perrin IJ, Hayhurst DR (1994) Creep constitutive equations for a 0.5Cr-0.5Mo-0.25V ferritic steel in the temperature range 600–675°C. J Strain Anal Eng Des 31(4):299–314

Polcik P (1999) Modellierung des Verformungsverhaltens der warmfesten 9–12% Chromstähle im Temperaturbereich von 550–560° C. Dissertation, Universität Erlangen-Nürnberg, Shaker Verlag Aachen

Polcik P, Straub S, Henes D, Blum W (1998) Simulation of the creep behaviour of 9–12% CrMo-V steels on the basis of microstructural data. In: Strang A, Cawley J, Greenwood GW (eds) Microstructural stability of creep resistant alloys for high temperature plant applications. Cambridge University Press, Cambridge, pp 405–429

Polmear IJ (1996) Recent developments in light alloys. Mater Trans, Jpn Inst Met 37(1):12–31

Polmear IJ (2004) Aluminium alloys—a century of age hardening. Mater Forum 28:1–14

Prager W (1956) A new method of analyzing stresses and strains in work-hardening plastic solids. J Appl Mech 23(4):493–496

Rabotnov YN (1959) O mechanizme dlitel'nogo razrusheniya (A mechanism of the long term fracture, in Russ.). Voprosy prochnosti materialov i konstruktsii, AN SSSR pp 5–7

Rabotnov YN (1963) O razrushenii vsledstvie polzuchesti (On fracture as a consequence of creep, in Russ.). Prikladnaya mekhanika i tekhnicheskaya fizika 2:113–123

Rabotnov YN (1969) Creep problems in structural members. North-Holland, Amsterdam

Raj SV, Iskovitz IS, Freed AD (1996) Modeling the role of dislocation substructure during class M and exponential creep. In: Krausz AS, Krausz K (eds) Unified constitutive laws of plastic deformation. Academic Press, San Diego, pp 343–439

Reddy JN (1997) Mechanics of laminated composite plates: theory and analysis. CRC Press, Boca Raton

Reiner M (1969) Deformation and flow. an elementary introduction to rheology, 3rd edn. H.K. Lewis & Co., London

Rice JR (1978) Thermodynamics of the quasi-static growth of griffith cracks. J Mech Phys Solids 26(2):61–78

Riedel H (1987) Fracture at high temperatures. Materials Research and Engineering. Springer, Berlin

Roesler J, Harders H, Baeker M (2007) Mechanical behaviour of engineering materials: metals, ceramics, polymers, and composites. Springer

Schmicker D, Naumenko K, Strackeljan J (2013) A robust simulation of direct drive friction welding with a modified carreau fluid constitutive model. Comput Methods Appl Mech Eng 265:186–194

Schmicker D, Paczulla S, Nitzschke S, Groschopp S, Naumenko K, Jüttner S, Strackeljan J (2015) Experimental identification of flow properties of a S355 structural steel for hot deformation processes. J Strain Anal Eng Des 50(2):75–83

Skrzypek J, Ganczarski A (1998) Modelling of material damage and failure of structures: foundation of engineering mechanics. Springer, Berlin

Straub S (1995) Verformungsverhalten und Mikrostruktur warmfester martensitischer 12%-Chromstähle. Dissertation, Universität Erlangen-Nürnberg, VDI Reihe 5, Nr. 405, Düsseldorf

Szilard R (1974) Theory and analysis of plates. Prentice-Hall, Englewood Cliffs, New Jersey

Timoshenko SP, Goodier JN (1951) Theory of elasticity. McGraw-Hill, New York

Timoshenko SP, Woinowsky-Krieger S (1959) Theory of plates and shells. McGraw-Hill, New York

Wagner C (1961) Theorie der Alterung von Niederschlägen durch Umlösen (Ostwald-Reifung). Zeitschrift für Elektrochemie, Berichte der Bunsengesellschaft für physikalische Chemie 65 (7–8):581–591

Xiao H, Bruhns OT, Meyers A (2006) Elastoplasticity beyond small deformations. Acta Mech. 182(1–2):31–111

Zhang J, Deng Y, Zhang X (2013) Constitutive modeling for creep age forming of heat-treatable strengthening aluminum alloys containing plate or rod shaped precipitates. Mater Sci Eng: A 563:8–15

Ziegler H (1983) An introduction to thermomechanics. North-Holland series in applied mathematics and mechanics, vol 21, North-Holland, Amsterdam